Johnsson Matthey

Monolithic Pt & Pd catalyst

Method for development of Pt & Pd monolithic catalyst in FORMOX™ ECS unit

Emil Gammelgaard
9-17-2018

Abstract

FORMOX™ is a formaldehyde production process, utilizing a metal oxide catalysts. The new generation of plants is pressurized, therefore the turbo charger concept has been developed. This concept deploys a turbine coupled to a compressor, where the turbine recovers a substantial part of the electric power needed to run the compressor, from the outlet of the emission control system unit (ECS) in the process. The ECS needs to operate with a lower pressure drop over the catalyst bed, for the turbocharger to reach its full potential. The present studies main objective is to make a comparison between the two different geometries and test several samples under different conditions to compare; light off temperatures and slip values. This work will lay the groundwork for a technical support method which will help Johnsson Matthey (JM) and its customers to predict life span- and emission from ECS catalysts. The results show that the monolith structure is more active and has a lower amount of slip than the pellet catalyst previously used. A mixture of Pt and Pd is also advantageous compared with a pure Pt monolith, and increases the activity further. Costumer trials show a correlation between catalyst operation time and activity, but no correlation between operation time and slip values.

Acknowledgement

First, I would like to thank the JM R&D team for their hospitality and expertise. It has been a privilege to tap into their knowledge and experience in all aspects of this project.
Special thanks to Alina Moscu - my main supervisor during this project. Thank you for your patience, the laughs and for being my coach in my first 10 km run.
I would also like to thank the team on Perstorp AB R&D for all the fika and for teaching me about; the chemistry concerning house pools, and the optimal diameter of a barbecue grid when serving **n** guests. Engineering truly has many uses.
I would also like to thank my mother for letting me stay with her all summer, and Anna Olofsson for all mental support and believing in me when I doubted.
Lastly I would like to thank Chistian Hulteberg for the service as institution supervisor, and Per Tunå for examining my project.

Abbreviations and chemical compounds

CPSI – Cell Per Square Inch

DME – Dimethyl Ether

ECS – Emission Control System

FID – Flame Ionization Detector

GC – Gas Chromatography

GHSV – Gas Hourly Space Velocity

IR – Infrared detector

JM – Johnsson Matthey

MFC – Mass Flow Controller

MR – Measuring range

PID – Proportional Integral Derivative controller

PLC - Programable Logic Controller

Pd – Palladium

PPM – Part Per Million

Pt – Platinum

RDS – Rate Determining Step

VOC – Volatile Organic Compound

Table of Contents

Abstract i
Acknowledgement ii
Abbreviations and chemical compounds iii
1.0 Introduction 1
1.1 Background 1
1.2 Project objective and aim 1
2.0 Theory 3
2.1 Historical Background 3
2.2 **FORMOX™** Formaldehyde production 3
2.3 Pellets- and monolithic supports 5
2.4 Support material 5
2.5 Active component 6
2.6 The Langmuir Theory of Adsorption 6
2.7 Reaction Mechanisms 7
2.8 Catalyst deactivation 7
2.9 Catalytic oxidation reaction theory 8
3.0 Experimental method, materials and setup 11
3.1 Pilot setup overview 11
3.2 Calibration 12
3.2.1 Coriolis flow meter 12
3.2.2 MFC Calibration 12
3.2.3 **ULTRAMAT™** 23 IR calibration 13
3.2.4 **FIDAMAT™** 6 calibration 14
3.2.5 GC calibration 14
3.3 Catalysts 15
3.3.1 Specification 15
3.3.2 Insertion method 16
3.4 Experimental methods 16
3.4.1 Light off test 16
3.4.2 Slip test 17
4.0 Results 19
4.1 Light off curves 19
4.2 Slip values 22
5.0 Discussion 28
5.1 Light off comparison 28

5.2 Slip comparison 29
5.2 Experimental uncertainty and sources of error 29
5.3 Method suggestion 30
5.4 Future work 31
6.0 Conclusion 31
Appendix 32
A. Pilot process sheet 32
B. Methanol solution preparation 35
C. Coriolis calibration data 36
D. MFC calibration data 37
E. Calibration gases used for calibration in the gas chromatograph 39
F. Average peak areas and the corresponding concentration linearization in figures 40
G. Catalyst geometry calculations 43
References 44

1.0 Introduction

In this project, different catalysts for oxidizing formaldehyde production off- gasses will be tested in a pilot. The catalysts will be tested with different inlet gas compositions, gas hourly space velocities (GHSV) and bed temperatures. A thermal aging method will also be done to compare fresh and aged samples, and these samples in turn will be compared to JM costumer samples, which has been used in real scale plants

1.1 Background

A recent invention integrated in the **FORMOX™**™ process is the turbocharger concept. This includes a turbine connected to a compressor, which allows the formaldehyde producers to recover almost all energy required to pressurize the plant.

The ECS is in place to clean the process off-gas, by catalytically oxidizing the trace hydrocarbons in the off-gas into water and carbon dioxide. The catalyst in the ECS is currently in a packed bed configuration, with the catalyst itself being spherical alumina supports with platinum (Pt) and palladium (Pd) as the active material. Following the turbocharger concept introduction, a new ECS technology is needed due to the increased pressure drop over the catalyst bed.

Honeycomb monolithic technologies have been found to be a promising alternative to the current packed bed due to their low pressure drop and high resistance to plugging.

JM has therefore invested in a pilot plant which resembles the ECS in the **FORMOX™** process. Here, catalytic oxidation of a typical plant off- gas mixture is studied, and the combustion gases is measured on with an online Flame ionization detector (FID) (Siemens **FIDAMAT™**), Infrared detector (IR) (Siemens **ULTRAMAT™**) and gas chromatography (GC) (SRI **model 8610C Gas Chromatograph™**).

This project is a continuation of a similar previous study (1) conducted by another JM employee. For this project two important upgrades have been done to the pilot equipment for further insight:

- Addition of a gas chromatograph for quantification of CO, CO_2, DME, MeOH and formaldehyde.
- Addition of designated formaldehyde solution tank, which enables formaldehyde to be in the reaction mixture.

1.2 Project objective and aim

The goal of this project is to gain a better understanding on the differences between monolithic- and pelletized Pt and Pd catalysts.

The objectives to achieve this goal are:

- Understanding the behavior of the Pt and Pd based catalysts under gas mixtures typically observed at plant scale in the ECS reactor.
- Testing of Pt and Pd pellets and honeycombs at various conditions (different space velocities, gas compositions and temperatures) to enable development of a standard method that will serve as a base for technical support service to help customer predict the end of the catalyst life time and emissions produced.

To achieve these objectives a literature study must be carried out to understand the behavior of Pt and Pd honeycomb and pellet catalysts under conditions similar to those used for the project. To operate the pilot system, calibration of all analytical- and mass flow equipment needed to be made. Before any real experiments can be made, blank tests must be made to verify the temperature control inside the reactor. The experiments should determine the catalyst behavior in the presence of a single- and multi-component gas feed, where the latter should consist of gases that are usually found at the ECS reactor inlet. Verify the influence of the formaldehyde in the reaction mixture during slip experiments and test the catalyst activity at different space velocities. If time allows, testing of spent samples from several customers to be used as a validation for the testing method. Draw conclusions and establish a standard method for the Pt and Pd pellet and honeycomb catalysts to be used for testing of samples received from customers. This should allow prediction of catalyst lifetime and estimate the emission level at different stages of the catalyst lifetime.

2.0 Theory

The structured catalysts commercial breakthrough is summarized in historical background before the theoretical models and concepts used in catalytic oxidization is presented. The **FORMOX™** process is also briefly introduced, to give the reader a picture of the industrial scale, which this study seeks to mimic a pilot of.

2.1 Historical Background

Monolithic- or honeycomb catalysis gained commercial interest in the USA after the 1967 Federal Clean Air act, which required all 1968 model year vehicles to meet new emission standards. Several engine modifications where made by the producers to meet the new requirements, but with heavy penalty to the vehicles performance, and fuel economy. Ford and General Motors initiated studies to examine the relative deactivation rate of catalysis in the afterburner of their exhaust systems, and concluded that when operated on unleaded gasoline, noble-metal catalysts would be feasible. In 1970 the General Motors president told the American Petroleum Institute of his intentions to install catalytic converters on all new vehicles by 1975, which would require unleaded gasoline. (2)

These events initiated the commercial interest in catalytic conversions of exhaust gases, later called three-way catalyst (3). The Corning Co. developed the cordierite ceramic support which is used in 95% (2) of today's converters. These at the time newly developed catalytic converters used both pellet- and monolithic geometries.

2.2 FORMOX™ Formaldehyde production

To get an idea of which pollutants is present in the ECS inlet stream, a short description of the **FORMOX™** process plant follows.

The production of formaldehyde are carried out by the following two reactions (4):

$$CH_3OH \rightleftarrows CH_2O + H_2 \quad \Delta_r H = 85\ kJ/mol \qquad \text{eq.1}$$

$$CH_3OH + \frac{1}{2}O_2 \rightarrow CH_2O + H_2O \ \Delta_r H = -158\ kJ/mol \qquad \text{eq.2}$$

The partial oxidation, eq. 2, is carried out over a metal oxide catalyst, and the heat generated drives the dehydrogenation reaction eq.1. Below in figure 1, a schematic representation of the **FORMOX™** process is displayed. Fresh and recycle methanol is mixed and evaporated in the vaporizer. Here, air is also introduced. The resulting gas is combined with steam and heated to the reaction temperature. The reactant gas is lead to the reactor, where the reaction occurs over a metal oxide catalyst. Once past the catalyst, the product gases are immediately cooled in a heat exchanger. The gases are introduced near the bottom of an absorber where water is sprayed from the top. Out of the bottom of this absorber the final product is collected, which is 37-55wt% formalin (formaldehyde solved in water) (4). There is also a small content of methanol which helps stabilize the formaldehyde, and prevents polymerization of the formaldehyde (5). Although selectivity toward formaldehyde is very high, several side reactions occur which by products is absorbed in the off gas that is the inlet to the ECS.

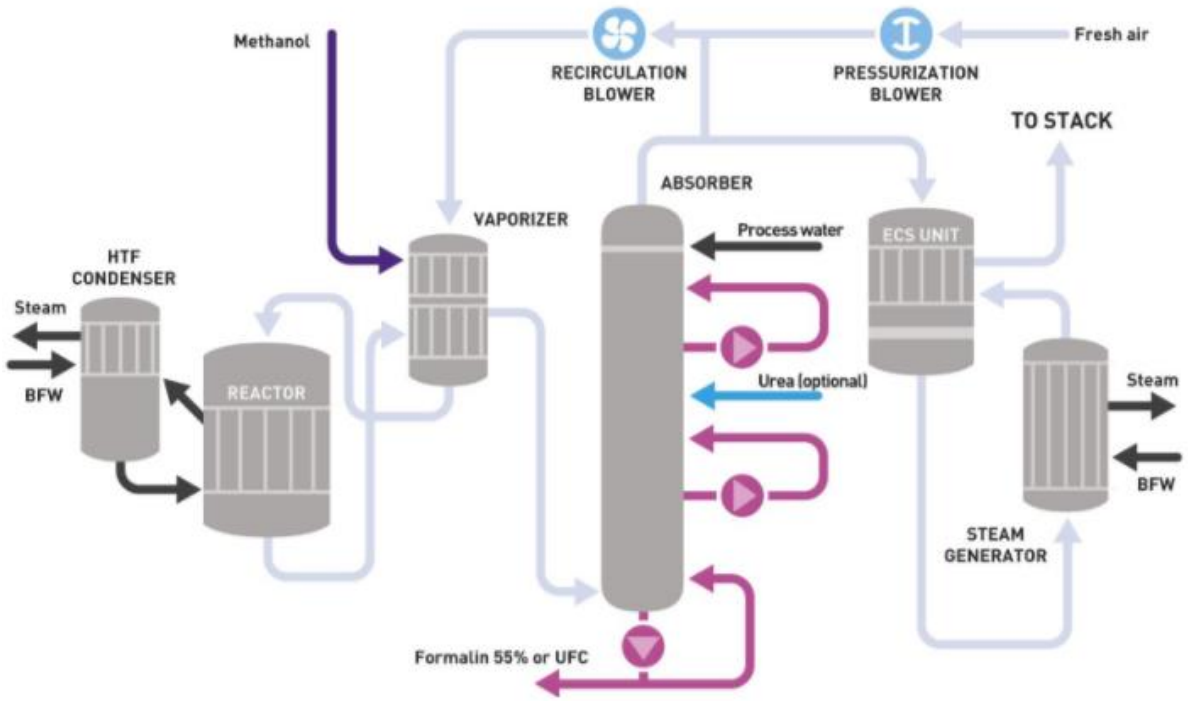

*Figure 1:The **FORMOX™** process. (6)*

Here, the gas containing mostly CO, N_2, O_2, CH_3OH, DME (dimethyl ether) and formaldehyde, is catalytically oxidized over a Pt/Pd-$\gamma - Al_2O_3$ catalyst. The turbocharger concept can be implemented to the presented process above according to the figure below:

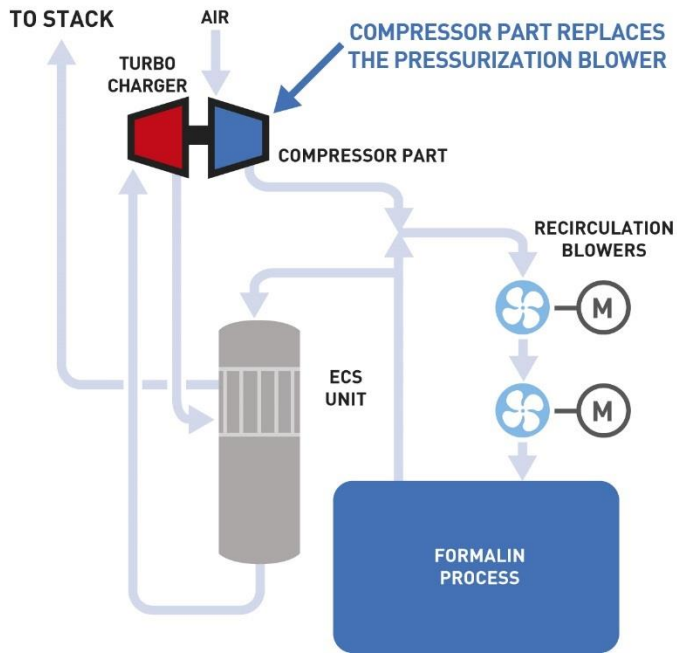

*Figure 2: The turbo charger concept, the **FORMOX™** process is represented here within the Formalin process block. (7)*

2.3 Pellets- and monolithic supports

Pellets, is a small spherical or cylindrical support structures with a vast amount of irregular micro pores in them (8). These pores walls have the active component distributed on them, there is also active sites on the spheres itself, and depending on whether the highest concentration of active component is within the interior- or the surface of the particle the type of pellet catalyst is referred to as “egg yolk” or “egg shell” catalyst respectively (8) . These spheres are usually packed in a cylinder with the right dimension, and properties, hence the name packed bed.

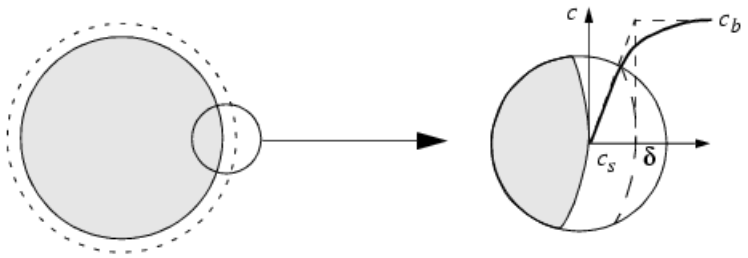

Figure 3: Catalyst pellet with boundary layer and a general representation of the bulk concentration of reaction species which decreases towards the surface. (9)

The monolithic support is a structured form of catalyst, consisting of many parallel straight or zigzag passages. The support material consists of metals, metal alloys or ceramic depending on the application. The active component can either be incorporated in the porous ceramic monolithic support structure so called incorporated monolithic catalyst. Or the active component can be applied as a coat on the walls in the monolithic support channels, so called washcoated monolithic catalyst (10). The main difference being that in the incorporated case, the mass-transfer of reactant has access to all channels through radial diffusion, for washcoat monoliths this is not the case (10).

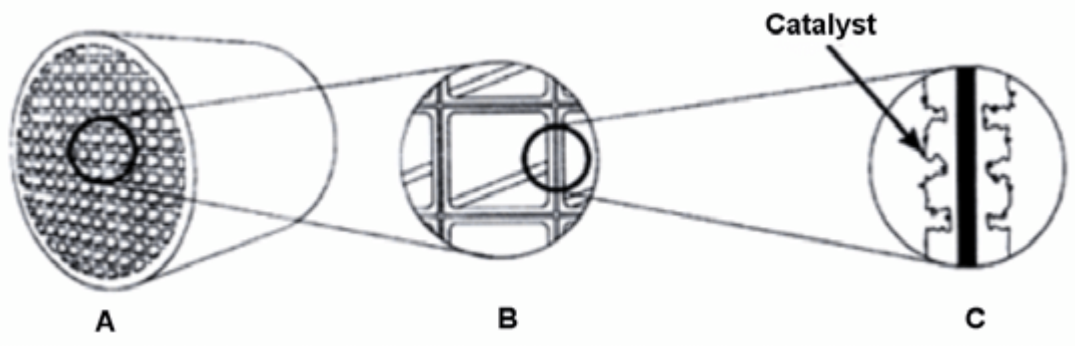

Figure 4: Monolith structure, with channels and dispersed active catalyst phase. (11)

The most outstanding advantage of monolithic catalysts when compared with packed bed pellets, is the reduced pressure drop over the bed (2), (10). Under optimal flow conditions the flow is evenly distributed in each monolithic channel, effectively eliminating temperature peaks “hot spots” along the profile, which is more likely to occur in randomly packed beds (10).

2.4 Support material

As stated above the material which the support consists of varies depending on the application. The main objective of the support, is to supply a durable base where the active component can be applied, and stay throughout the lifetime of the catalyst (8). The durability of the support is dependent on the following properties:

- Microstructure; meaning porosity, pore size distribution and microcracking tendency
- Coefficient of thermal expansion
- Strength; crush strength and modulus of rupture
- Structural modulus
- Fatigue behavior.

These properties are inherent for the material, but can also be altered in the production of the monolithic structure (2). A commonly used support for monolithic noble metal catalysis in industrial off- gas application is a washcoat of gamma alumina (γAl_2O_3), which is a porous stable material and typically has a surface area of 150-175 m^2/g. The gamma configuration of the material can however at high temperatures shift to the alpha configuration, which distorts the material and must be avoided (3). While γAl_2O_3 main function is as support, it can increase the metal oxides redox activity, thus enhance it through increased lattice O_2 mobility (12), (13). This is a phenomenon which is defined as strong metal support interaction (SMSI) (14).

2.5 Active component

The three-way catalyst commercially invented as an automotive exhaust catalyst (2), (3), removes the three main pollutants from a combustion engine which is CO , NO and unburned hydrocarbons with the following overall reactions (3):

Table 1:Reactions in three-way catalysis

Reaction	*Catalyst*
$CO + 1/2O_2 \rightarrow CO_2$	Pt, Pd
$C_xH_{2x+2} + yO_2 \rightarrow xCO_2 + zH_2O$	Pt, Pd
$2NO + 2CO \rightarrow N_2 + 2CO_2$	Rh, Pd

From table 1 it can also be noted which active component that contributes the most to the specified reaction.

2.6 The Langmuir Theory of Adsorption

When studying heterogeneous catalytic oxidation reactions, the Langmuir Theory of Adsorption is fundamental. An introduction follows, derived as presented in Herbschleb C. T. Doctoral thesis (15). And later also a basic definition of the reaction mechanics from this same thesis.

In any catalytic reaction, the reactants must interact with the catalyst through a process called adsorption. Two kinds are possible; associative- and dissociative adsorption. In the latter case, the adsorbate molecules bond most be broken when adsorbed. In associative adsorption, this is not the case. The assumptions for this theory is as follows:

- The solid surface is uniform, and consists of equivalent sites, which can be occupied by only one gas molecule.
- The equilibrium between the gas and adsorbate state is dynamic.
- When a gas molecule collides with the surface and hits an empty site, it is bonded; otherwise it is reflected.
- Adsorbed molecules are localized

The fractional coverage, ϑ_i of a compound, i, on the catalyst surface is defined as the number of sites the compound occupies divided with the total number of sites on the surface:

$$\vartheta_i = \frac{N_i}{N_{tot}} \qquad \text{eq. 3}$$

In the case of this study, the reaction is in the gas phase, so ϑ_i depends on the pressure. Hence the adsorption rate and desorption rate can be defined for an associative adsorption:

$$r_A = k_a \cdot p \cdot (1 - \vartheta) \qquad \text{eq.4}$$

$$r_D = k_D \cdot \vartheta \qquad \text{eq. 5}$$

Where k_a and k_D are the adsorption and desorption kinetic constant, respectively. $(1 - \vartheta)$ is the relative density of free sites on the surface. Equilibrium is defined as when $r_A = r_D$ rewriting results in the Langmuir Adsorption Isotherm:

$$\vartheta_i = \frac{K \cdot p}{K \cdot p + 1} \qquad \text{eq. 6}$$

$$K = \frac{k_A}{k_D} \qquad \text{eq.7}$$

Dissociative adsorption can be derived in the same way and results in the following Langmuir Adsorption isotherm:

$$\vartheta_i = \frac{\sqrt{K' \cdot p}}{1 + \sqrt{K' \cdot p}} \qquad \text{eq.8}$$

2.7 Reaction Mechanisms

When studying catalytic oxidation of VOCs two different reaction mechanisms is frequently used; The Langmuir – Hinselwood- and the Mars Van Krevelen mechanism.

In the Langmuir – Hinselwood mechanism, both VOC and O_2 must adsorb to the surface of the catalyst. Then, the adsorbed reactants react and the product is directly desorbed from the surface to the gas phase.

In the Mars-Van Krevelen case the partial pressure of oxygen needs to be high to get a high fractional coverage of O_2. The VOC will then react directly from the gas-phase with the adsorbed O^- on the surface to produce oxidized products. The reaction rates of these two mechanism can be derived from the Langmuir Isotherms, and are as follows:

$$R_{LH} = k \cdot \vartheta_{VOC} \cdot \vartheta_{O_2} \qquad \text{eq. 9}$$

$$R_{MK} = k \cdot \vartheta_{O_2} \cdot p_{VOC} \qquad \text{eq.10}$$

When R_{LH} is written in this way, the reaction between reactants on the surface is the rate determining step (RDS), and k is the reaction constant for this reaction.

2.8 Catalyst deactivation

Catalyst deactivation is central to the objective of this project, as well as to JM and its customers. In this section a brief description of catalyst deactivation will be done. Many phenomena are responsible for a catalysts inevitable loss of activity. Here, two deactivation phenomena will be described which is of concern.

Poisoning is a phenomenon where a chemical compound adsorbs strongly to the active site, preventing relevant reactant species to adsorb to the catalyst surface (16). The compound need only have an affinity to the active site higher than that of the real reactant, and keep this affinity within the process temperature interval to act as a poison in the context. When the compound Is

chemisorbed at the surface, it effectively blocks a varying number of adjacent sites physically, but can also alter the electronic or structural geometry of the surface (16).

Sintering, is a thermal induced deactivation phenomenon caused by loss of catalytic phase area. The area is reduced when small catalytic particles merge together because of much increased particle migration when temperature is >500 ℃ (16). The support structure can also partially collapse causing less active area of the catalyst, this is also induced by elevated temperatures under long periods of time.

Both deactivation mechanisms are accountable for the loss of activation sighted in the costumer samples which has been studied in this project.

2.9 Catalytic oxidation reaction theory

The compound most abundant in the off- gas is CO. The catalytic oxidation of carbon monoxide has been diligently studied since the 1970s.

$$CO \quad + \frac{1}{2} O_2 \rightarrow \ CO_2 \qquad \text{eq. 11}$$

The reaction is proposed to follow a Langmuir Hinshelwood mechanism when catalysed by a Pt/Pd-γAl_2O_3 catalyst, where CO and O_2 compete for the same sites (17), (18), (19), as follows:

Associative adsorption of CO

$$CO + M \ \rightleftharpoons CO - M \quad \text{eq. 12}$$

Dissociative adsorption of O_2

$$O_2 + 2M \rightleftharpoons 2\ O - M \quad \text{eq. 13}$$

Surface reaction

$$CO - M + O - M \rightarrow \ CO_2 + 2M \quad \text{eq. 14}$$

Where M is an active component, Pt or Pd in this case. There is no unilateral implication of which of these reactions is the RDS. According to Depcik *et. al* (20) most authors either treat the dissociative adsorption of oxygen, eq. 13, or the surface reaction between adsorbed species, eq. 14, as rate determining, depending on the carbon monoxide concentration. When CO concentration is low eq. 14 is the RDS and when the concentration of CO is high eq. 13 is the RDS. The RDS also depends on the M – O bond energy, if the energy is high eq. 14 is the RDS, and if it is low eq. 13 is the RDS (14).

Oxygen adsorption is considered the RDS due to its dissociative adsorption nature. When oxygen diffuses to the surface and along the surface, it must find two adjacent reaction sites for the adsorption to take place (17). This combined with the fact that the oxygen sticking coefficient (0.02 – 0.05) is considerably lower than that of CO (0.2-0.8) (17), makes oxygen adsorption the limited step in this application.

Pt, Pd bimetallic catalyst application in catalytic CO oxidation where studied by J. M. Hazlett *et. al* (21). They concluded that with a higher ratio of Pd in the catalyst, lower activation in CO oxidation was observed due to a difference in how the CO binds to the active component surface. To high Pd content however lead to the formation of carbonate on the surface, inhibiting the active sites. To high Pt ratio made the active sites more prone to CO poisoning, due to Pts higher bond strength with

CO. The conclusion being that if a bimetallic alloy is to be used in catalytic oxidation of CO, then a 1:1 PtPd ratio is preferred, in high reactant concentration applications.

Methanol oxidation is a more complicated reaction mechanic involving several reactions occurring at the catalytic surface. The most common reactions are presented and discussed by Pan *et. al* in their study of SMSI in heterogeneous catalysis (14). The elementary reaction steps are generally believed to happen on the catalytic surface during methanol oxidation:

Dehydrogenation reaction of methanol on surface

$M - CH_3OH \rightarrow M - CO + 4H^+ + 4e^-$ eq.15

Water dissociation reaction

$M - H_2O \rightarrow M - OH + H^+ + e^-$ eq.16

CO oxidation reaction

$M - CO + M - OH \rightarrow CO_2 + H^+ + e^-$ eq.17

The dehydrogenation of methanol on the surface generates more CO on the surface effectively preventing methanol adsorption. This effect can be minimized when Pt is alloyed with Rh (14), the reaction path then bypasses eq. 15 and the surplus CO is avoided. In addition, when Pt is supported on γAl_2O_3, electronic effects between the active component and support induces metal particle motion or metal particle tilting resulting in the formation of SMSI. This effectively reduce the strength of the Pt-CO bond, thereby enhancing methanol oxidation (14).

DME partial oxidation on alumina supported noble metal catalysts was studied by Wang. S , Ishihara T. and Takita Y. (22). The decomposition of DME on the catalyst surface follows:

$CH_3OCH_3 \rightarrow CH_3O - Pt + CH_3 - Pt$ eq.18

$CH_3O - Pt \rightarrow CO - Pt + 3H - Pt$ eq.19

$CH_3 - Pt \rightarrow C - Pt + 3H - Pt$ eq.20

$CH_3 - Pt + H - Pt \rightarrow CH_4 - Pt$ eq.21

$H - Pt \rightarrow 1/2H_2 - Pt$ eq.22

$C - Pt + 1/2O_2 \rightarrow CO - Pt$ eq.23

It is evident that larger components like methanol and DME requires many steps to be fully oxidized in the ECS reactor, which implies that the partial oxidation of DME is likely to produces several different compounds. Wang S. *et. al* (22) analysed the oxidation products of DME partial oxidation over $\gamma - Al_2O_3$ supported Pt catalysts at 450 °C with the following results:

Table 2:Partial oxidation products, results from Wang. S et al. [17] study.

	$\gamma - Al_2O_3$[Pt]
Conversion of DME %	85
Selectivity %	-
- CO	36
- H_2	15
- CH_4	41
- HCHO (formaldehyde)	16
- CO_2	7

These results imply that two different paths to formaldehyde slip can be expected from the ECS system. First, product formaldehyde which passes the ECS unreacted. Second, DME partial oxidation product.

Few mechanisms of formaldehyde oxidation have been reported in literature (23). Several mechanisms based on Mars Van-Krevlen has been proposed. Below a formaldehyde oxidation mechanism on a Pt- and Pd – TiO_2 catalyst is presented (23) which should bear much resemblance to the same reaction on $\gamma - Al_2O_3$:

$$HCHO + O - M \rightarrow H_2CO_2 - M \rightarrow CO - M + H_2O \qquad eq.24$$

The carbon monoxide reacts then according to eq. 14 or eq. 17 above, depending on which species interacts with the CO. The decomposition of formate species to CO on the surface is the rate limiting step in this mechanism.

With all these reaction mechanisms presented above, a meaningful hypothesis of how the reaction series of the compounds in a mixture will turn out is impossible to make. Rather, a black box study of the ECS will be evaluated.

3.0 Experimental method, materials and setup

In this title, the pilot system will be described to give the reader a general idea, a full detailed description of the ECS pilot can be found in appendices A and B. The method for calibrating all the instruments also has its subchapter. The catalyst material is specified, as well as the method for insulating the bed, once in place in the reactor cylinder. The different experimental methods used with the pilot is also described.

3.1 Pilot setup overview

The dosing system of the pilot consists of one mass flow controller (MFC) for each supplied gas and two Coriolis pumps which delivers methanol- and formalin solution. The gases and liquids are preheated before they are mixed and vaporized in the vaporization unit. The vaporizer unit heater controls the reactor inlet temperature. Once the liquids are vaporized and mixed with the other gases, the reaction mixture continues either to the reactor, or through the bypass directly to the analytical section.

The reactor is a metal cylinder which holds a catalyst cylinder which has an inner diameter of 40 mm. In this catalyst cylinder, either monolith- or pelletized catalyst is inserted, along with a tight layer of ceramic cloth, which works as isolation, to prevent slip of reaction gases along the reactors sides. For this project a bed height of 140 mm has been chosen. The reactor also has heavy isolation on the outside which makes the setup approximately adiabatic.

After the reactor, the main part of the exhaust is lead to the stack, but a fraction -how much is adjusted with a valve- is taken to the analytical section. Here the exhaust gases first passes through the online FID. The FID works by leading the gases towards a hydrogen and air fuelled flame. The organic carbons will combust and some of these carbons will produce ions which generates a current that is quantified, and converted to a signal which is proportional to a substance concentration. In this way, the FID measures a total organic carbon signal, and does not distinguish between substances.

The IR is in place to measure CO concentration in the exhaust gas. The basic principle of measurements consists of a IR light source emitting light through a sample chamber, where the sample gas is continuously flowed. Here the CO will absorb light on the given frequency and reemit it with a new lower intensity. The difference between these light intensities is the substance absorbance, which is proportional to the concentration. The signal is converted to CO concentration which is monitored and recorded continuously.

A fraction of the exhaust is taken by a separate isolated pipe to the GC. Here valves are in place to adjust the gas flow into the GC, as well as heater which makes sure no condensate is injected to the GC. The flow can visually be estimated since the outlet of the GC pipe is situated under water in a sealed beaker. This means that bubbles can be seen leaving the exhaust pipe at a certain rate, and the operator can set the gas flow by adjusting the valves and see the change in bubble rate. The sealed beaker also has an exit pipe leading to the stack. The GC has two porous polymer columns each with a different detector. One detector is an FID with principle of measurement as described above. The other one is a methanizer FID. Once the carbon-based substances elute from the column they pass a nickel catalyst in a heated chamber where they are hydrogenated to methane, which is combusted in the FID by the same principle as described above and measured. Since the substances have different retention times from the column they can be separated and quantified by integrating their time-absorbance response.

The pilot is controlled via a Programable Logic Controller (PLC), which is accessed by the operator on a stationary computer. Here flows, temperatures, pressures and analytical instruments signal is recorded, and can be monitored in real time. This PLC also has a programable sequence sheet, where process times can be set for specific process variables.

All temperatures in the system is controlled with a proportional-integral-derivative controller (PID). Basically, this works as follows: A set point is set in the PLC, from a thermocouple the PLC receives a signal with the actual process temperature, called the process value. The difference between the set point and process value is calculated. Based on the magnitude of the difference and for how long it has been in effect, a signal is sent to the heater which heats up the system, thereafter the procedure is carried out again.

3.2 Calibration

All the analytical instruments and dosing instruments needs calibration before experiments can be conducted. In this section the different unit calibrations will be summarized.

3.2.1 Coriolis flow meter

There is two Coriolis flow meters in the pilot system. One for methanol solution and one for formalin. A specification of the units is presented in a table below, the exact position of the units can be seen in appendix A:

Table 3: Coriolis unit specification with properties and flown substances.

Unit name	Solution [wt%] (distilled water as balance	Max flow [g/min]	Min – max [Bar(g)] inlet pressure
CFM902:01	Methanol, 5 *	15.0	1 – 3.5
CFM902:02	Formaldehyde, 37 Methanol, 12.4 **	0.250	1 - 3

**Methanol solution was prepared according to appendix C.*
*** Formaldehyde solution was bought from Sigma Alderich, and exact concentration was measured by on-site lab.*

The procedure used to calibrate these units is as follows:

1. The outlet of the Coriolis is disconnected from the pilot system and lead to a cylinder which empty weight is measured.
2. A certain flow is set on the PLC and a timer is set when the first drop lands on the cylinder bottom.
3. The flow is maintained for approximately 60 min for the first low flows and less time for the higher.
4. When the timer expires, the weight is measured again, and the difference is divided with the measured time interval.

This procedure is repeated for several flows distributed evenly on the Coriolis flow capacity spectrum and the actual mass flow is plotted vs. the PLC set point. In this way, a linear function is created, where the slope is the deviation factor. For the full data set and linear functions see appendix D.

3.2.2 MFC Calibration

The gas MFCs calibration method is theoretically the same as the Coriolis calibration. They differ in practice due to the different states of aggregation. The procedure requires a second flow meter which is installed downstream of the MFC controller which is being calibrated. Three different flow

meters is needed due to the difference in capacity between the MFCs. See specification of pilots MFCs below:

Table 4: MFC unit specification with properties and substances.

Unit name	Substance	Max flow [nL/min]	Min – max [Bar(g)] inlet pressure	Correction factor
MFC902:01	Air	50	0 - 4	1
MFC902:02	Nitrogen	200	0 – 4	1
MFC902:03	DME	1	0 - 3	0.4088
MFC902:04	CO	5	0 - 5	1

The following procedure describes MFC calibration:

1. The flowmeter was connected downstream of the MFC.
2. Air was flowed through the MFC with a specific set point.
3. Either the operator did an average of a 2 min reading (Air, and nitrogen calibration) or the device performed 10 sequential readings and calculated the average automatically (CO and DME).
4. The acquired set points and their actual values are plotted in figures (see appendix D for full documentation), and the slope of the linear function is used as a correction factor for the inputs in the PLC as with the Coriolis.

Nitrogen and CO flows approximately as air through the MFC. DME however need additional correction for the calibration to resemble DME when it is done with air.

3.2.3 ULTRAMAT™ 23 IR calibration

The device has two measuring ranges (MR), MR1 which is for accurate measurement below 250 PPM and MR2 which is less accurate but has a higher range 250 – 10 000 PPM. One calibration point is needed for each range. The **ULTRAMAT™** has a one-point calibration method for the MRs, and automatic zero-calibration with ambient air. The table below specify the calibration parameters for each MR:

Table 5: Calibration parameters for each MR, the full calibration gas specification can be found in appendix D

MR	Span [PPM]	Calibration point [PPM]	Calibration gas [#]	Inlet Pressure [barg]	Inlet Flow [L/min]
1	0 – 250	100	12	0.1	1.2
2	250 – 10 000	10 000	5	0.1	1.2

The procedure for calibrating is:

1. Set the calibration point concentration, in the instruments calibration menu.
2. Connect calibration gas with the set concentration.
3. Wait for the measured value to stabilize.
4. Press calibrate.

The **ULTRAMAT™** is very stable, and the calibration remains valid over long periods of time. This was tested by checking the signal generated from the instrument when reconnecting the calibration gases two weeks after calibration. The values were on point! It has also been noted that the calibration points are independent of inlet pressure and flow, since the flow and pressure for the

inlet has been changed several times during the project, and the calibration has been stable during these changes.

3.2.4 FIDAMAT™ 6 calibration

This instrument detection mechanism is dependent on inlet- flow and pressure, and responds with variated amplitude to different components. Therefore, it is important to use a calibration gas which is the main constituent detected with this instrument during experiment. DME was used for span calibration. The instrument has three different measuring ranges which can be calibrated simultaneously if the total calibration is enabled, which is the case for this project. A zero calibration is also done with ambient air in the pilot which does not contain any detectable substance. The span calibration is done with a gas mixture from the pilot containing a known concentration of DME, in this case 5660 PPM. The set MFC flow is presented in the table below, the high air flow of the total calibration is because the DME MFC is unstable in the lower end of its operation span.

*Table 6: Gas flow through the pilot system for calibration, inlet conditions to the **FIDAMAT™** instrument is also presented.*

Calibration	Flow Air [L/min]	Flow DME [L/min]	Total flow [L/min]	FID inlet flow [L/min]	FID inlet pressure [bar(g)]
Zero	10	0	10	1.2	0.1
Total	150	0.85	150.85	1.2	0.1

The procedure for calibrating is:

1. Set the calibration point concentration, in the instruments total calibration menu.
2. Start MFC gas flow with the set concentration.
3. Wait for the measured value to stabilize.
4. Press calibrate.

3.2.5 GC calibration

The calibration of the GC was done with a collection of calibration gases specified in appendix D. The calibration gases where processed at least 10 times each for a reliable average of their absorbance. Then the absorbance and concentration was plotted and linearized, see appendix E. Worth mentioning is that the CO calibration is quite unreliable, but since the **ULTRAMAT™** is measuring the CO concentration continuously and very accurately, this is of no matter.

An attempt on calibrating the GC system to formaldehyde was also done. Formaldehyde was fed with the Coriolis, then vaporized and mixed with nitrogen in different ratios to obtain a calibration curve. Unfortunately, the formaldehyde and water in the solution is hard to separate by the GC column. Different GC oven-temperatures and temperature gradients was tested. But in every case the response peak was tailing very much, indicating two inseparable peaks in this case water and formaldehyde and no consistency in peak area could be obtained. It was decided that the project resources were insufficient to achieve a precise quantification of formaldehyde in the pilot system, and the calibration was discarded. Instead a one point calibration was attempted with 80 chromatograph runs on 1000 ppm formaldehyde fed, with the following results:

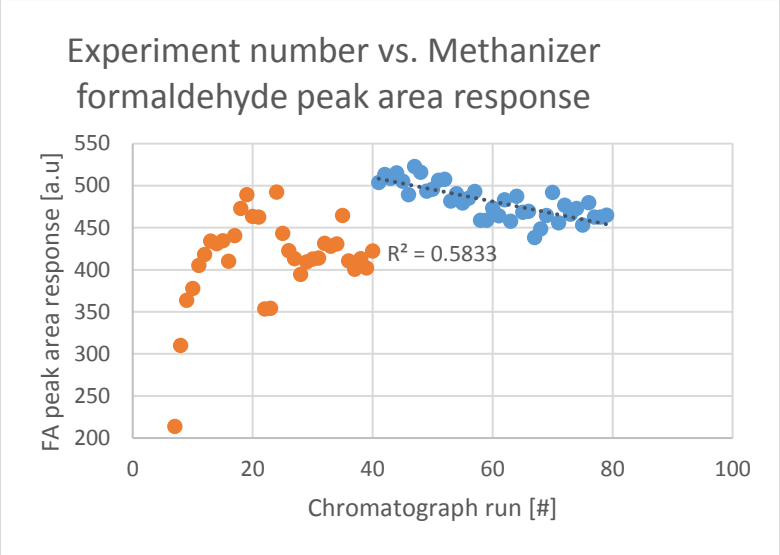

Figure 5: One point calibration of 1000 PPM formaldehyde concentration in pilot system. Peak area response in chromatograph is for each chromatograph run. Only >40 is used to estimate a linear fit, which is poor. The values vary in the interval 516 – 438 a.u.

Its concluded that no accurate formaldehyde concentration can be measured with the described method, and further recourses is needed if an accurate formaldehyde concentration is going to be quantified.

3.3 Catalysts

Here the specification of the catalysts is presented and the method for insertion into the reactor chamber, and insulation will be discussed. The exact amount of active phase on the catalysts is confidential but the catalysts load will be compared relatively.

3.3.1 Specification

As mentioned, two different geometries will be studied during this project; the pellet and the monolith. Here the different catalysts will be specified:

Table 7: Monolith (and reference P-Pt) catalyst specification. With L as space between monolith channels measured from wall centre, t is wall thickness, CPSI is monolith cell per square inch, OFA open frontal area is the fraction of the cross-section area which is available for the gas flow, GSA specific geometric surface area.

Specification	L [Inch]	t [Inch]	CPSI [cell/In^2]	OFA [%]	GSA [In^2/In^3]	Active phase	Active phase relative load:
P-Pt			d=4.7 mm pellet	-	9.43	Pt	3
M2-Pt	0.0659	0.007	230	0.80	54.2	Pt	2
M4-Pt	0.05	0.0065	400	0.76	69.6	Pt	2
M2-Pt:Pd	0.0659	0.007	230	0.80	54.2	Pt:Pd [1:3]	4

The catalysts above where all tested fresh. This means that they are either tested in the reactor for the first time, or has been tested on several times during the previous project (1). There has also been made a few tests on aged species of the above catalysts. The catalyst is considered aged when it has undergone a thermal aging program in a calcination oven. The fresh catalysts which has been

tested on a few times suffers a negligible amount of sintering and thermal aging during the regular test, and are therefore still considered fresh.

3.3.2 Insertion method

The single most contributing experimental error in this project is the wall effect. This phenomenon is when the reaction gas slips between the catalyst bed and the reactor cylinder, and thereby reaches the analytical instruments unreacted. This effect is significant when operating on high space velocities. To minimize this effect, proper insulation must be placed between the reactor cylinder inner diameter and the catalyst bed. The insulation used in this project is a ceramic cloth which is fitted around the monolith in several layers before squeezing the catalyst bed into the reaction cylinder, taking care that the cloth does not rip. When preparing a P-Pt catalyst bed, an equal amount of cloth is inserted into the reaction cylinder before inserting the catalyst. When the catalyst pellets are in place, pressure is applied on the catalyst bed top with a soft plastic hilt of a screwdriver to force the pellets to pack into the cloth, thereby decreasing the wall effect further.

3.4 Experimental methods

This title deals with the different experimental methods used in this project to gather the results. Two practical methods were used light off- and slip tests. These two different types of catalyst evaluation tests were conducted with varying operation conditions such as; inlet gas composition, type of catalyst, inlet- and bed temperature and gas hourly space velocity (GHSV). GHSV is the ratio between the volumetric inlet gas flow and the volume of the reactor, the advantage of dealing with gas flow and gas velocity in GHSV is that when compared with the size of the reactor, these properties are scalable when upgrading the evaluated process from pilot to full scale.

3.4.1 Light off test

The light off test is done to compare catalyst ignition temperatures for different types of catalysts, when operating the process with different operation variables as stated above. The catalyst must be heated to a minimum temperature, so the inlet reaction gas heat is spent activating the reaction rather than heating the catalyst itself, these temperatures vary depending on the expected light off temp of the catalyst. Practically, this is done with the three heaters within the reactor furnace which each is fitted with a thermocouple. The temperature needs to be stable and approximately equal in all three zones, to avoid temperature gradients and thereby uneven reaction profile in the catalyst. This flow is heated with the vaporizer to an appropriate temperature, approximately 50 °C below furnace temperature before entering the catalyst. When the inlet gas flow, and the catalyst furnace has reached the set temperature and are stable, the CO flow starts and a programmed temperature gradient of 2 $℃/min$ initiates increasing the inlet gas flow temperature. The CO concentration out of the bed is continuously monitored and recorded with the **ULTRAMAT™**. Once the temperature reaches the light off point which usually is some ten degrees above the furnace temperature, the **ULTRAMAT™** signal drops very fast to a few percent of the fed value and the experiment is ended a few minutes after. The following conditions where set for the light off experiments in this project:

Table 8: The different light off experiment carried out in this project.

Experiment	1	2	3
GHSV [h^{-1}]	22 000	50 000	22 000
CO concentration [vol %]	0.2	1	1
O_2 concentration [vol %]	5	5	5

These experiments were carried out on different combinations of the presented catalyst in section 3.3. Once the data is gathered, the inlet reactor temperature is plotted vs. CO consumption for all data points, which is calculated accordingly:

CO conversion calculation:

$$X_{CO} = \frac{C_{CO,in} - C_{CO,out}}{C_{CO,in}} \qquad eq.25$$

3.4.2 Slip test

Once the reaction is running, there is an interest in examining the outlet gas from the reaction bed. JM has some guaranties regarding slip of different compounds through the stack. A slip test is a way of verifying these guaranties by quantifying each compound that slips past the catalyst and compare which of the catalysts that preform best in avoiding this phenomenon. This experiment is carried out at higher temperatures than the light of test in the span 450 – 550 °C furnace temperature. The gas mixture in this experiment needs to mimic the real exhaust from the process as closely as possible, this projects gas mixture is presented below:

Table 9: Slip test reaction gas mixture. Assuming the vaporization produces an ideal gas.

Compound	Formula	Concentration [mol%]
Nitrogen	N_2	91.3
Oxygen	O_2	5
Water	H_2O	2
Carbon monoxide	CO	1
Dimethyl ether	C_2H_6O	0.5
Methanol	CH_3OH	0.12
Formaldehyde	CH_2O	0.07

The slip test is divided into three different sequences, as several furnace temperatures is of interest, between each sequence a heating sequence is carried out where only inert compounds is fed to the reactor, below the different measurement sequences is presented:

Table 10: Slip test sequences, and corresponding furnace and inlet gas temperatures.

Sequence	Furnace temp [°C]	Inlet gas temp [°C]
1	450	215
2	500	265
3	550	315

The procedure for carrying out the experiment is as follows. The first temperature in sequence one is reached and dwelled at for several minutes to stabilize while the inert species (nitrogen and air) in the reaction gas mixture is fed to the bed. When the temperature is stable, the whole mixture is fed and some more minutes is waited out for stability. Downstream, the GC sampling sequence is stared which includes ten measurements á 12 minutes. Therefore, the pilot system is held at sequence one for 120 minutes before the heating sequence is started to reach sequence two. Each heating sequence takes about 20 minutes resulting in 60 more minutes of total test time. Practically the whole test takes about eight hours, the last hour consists of stabilization waiting time as mentioned above, and some waste time which is bound to be included because the system must be manually taken to the next sequence since the GC measuring sequence also must be initiated manually.

Automatic sequence shifts would make this method more time efficient, and is left to further studies in this project. The **FIDAMAT™** instrument is also in place to measure the total organic carbon content of the outlet from the reactor. This instrument combusts all the organic carbons in the outlet, in this case methanol and dimethyl ether (formaldehydes response is very weak) and gives a total signal. This signal will be compared to the GC results to verify.

4.0 Results

Here the results of the project are presented under subtitles corresponding to the experimental method used. Light off curves and light off temperatures for 50 % conversion (sometimes also 98 %) for different process variables such as: CO concentration and GHSV.

4.1 Light off curves

In this section the light off experiments will be presented. Two different CO concentrations has been tested, and two different space velocities. The first light off trial was done with 0.2 vol% CO and GHSV at 22 000 h^{-1}.

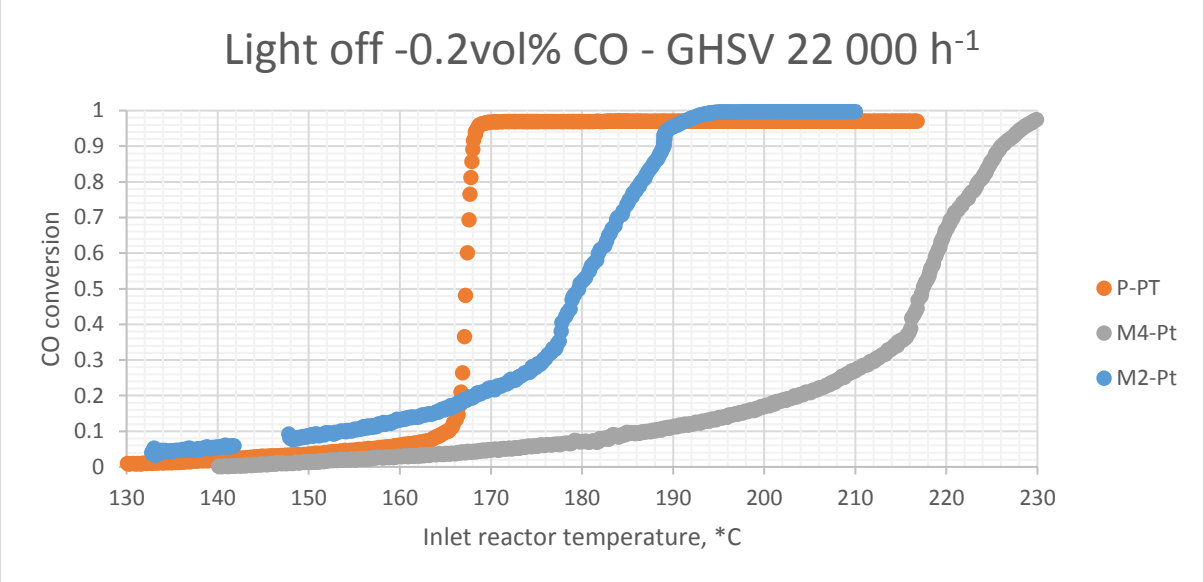

Figure 6: 0.2 vol% CO with an GHSV of 22 000 h^{-1}, the different catalysts runs is specified in the legend with name as presented in the 3.3 catalyst section

The curves above have the following T_{50} temperatures:

Table 11: Catalyst light of temperatures in centigrade for 0.2 vol% CO 22 000 h^{-1}, 50 and 98 corresponds to % conversion.

CATALYST	T_{50} [℃]	T_{98} [℃]
P-PT	167	170
M2- PT	180	192
M4-PT	217	203

These light off temperature will prove to be the lowest in this project for the catalysts individually, due to the low CO concentration in the reaction gas mixture. Considering section 2.9 eq. 13 - 14 when the CO concentration is low, more active sites will be available for the oxygen adsorption at lower temperatures. This means that the concentration of oxygen on the catalyst surface will be higher at lower temperatures, and the CO will react at these temperatures, effectively decreasing the light off temperature.

Next, the 1 vol% CO trial with GHSV 22 000 h^{-1} is presented, first the fresh run then the aged.

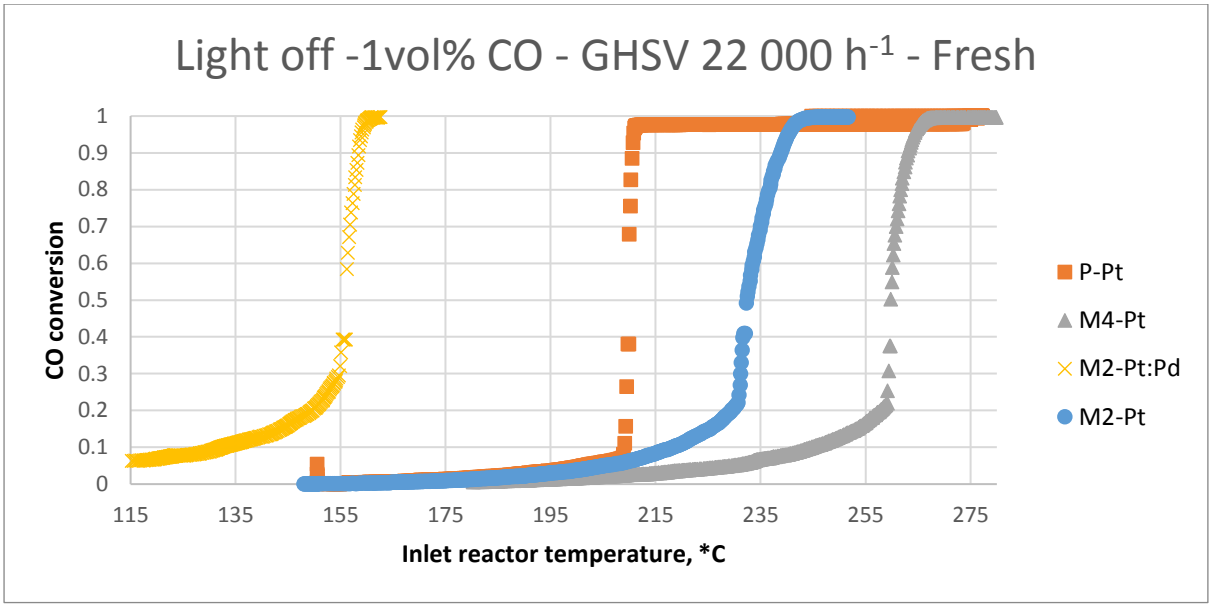

*Figure 7: 1 vol% CO with an GHSV of 22 000 h-1, the different catalysts runs is specified in the legend with name as presented in the 3.3 catalyst section. The data gap on the curves is due to the **ULTRAMAT™** switching measuring range.*

The curves above have the following T_{50} temperatures:

Table 12: Catalyst light of temperatures in centigrade for 1 vol% CO 22 000 h^{-1}, 50 and 98 corresponds to % conversion.

CATALYST	T_{50} [℃]
P-PT	210
M2-PT:PD	156
M2-PT	232
M4-PT	260

The aged 22 000 h^{-1} is presented below:

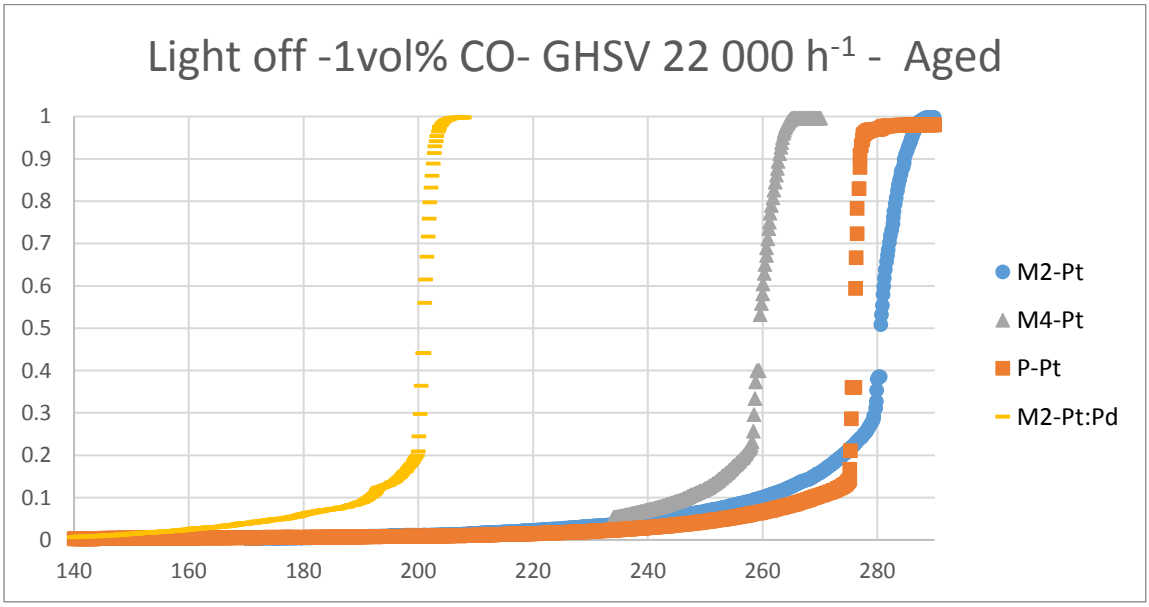

Figure 8: Light off curves for the aged catalysts. See section 3.3 for the ageing method.

A curious effect of ageing, is that M4-Pt light off is unchanged compared to the fresh trial, while the P-Pt, M2-Pt:Pd and M2-Pt suffers a 31 %, 29% and 21 % increase in T_{50} temperature respectively! See table below:

Table 13:Catalyst light of temperatures in centigrade for aged catalyst with 1 vol% CO, 22 000 h^{-1}. 50 and 98 corresponds to % conversion. The increase in T_{50} temp is compared with the fresh sample.

CATALYST	T_{50} [°C]	INCREASE OF T_{50} [%]
P-PT	275	31
M2-PT:PD	201	29
M2-PT	281	21
M4-PT	259	0

The 50 000 h^{-1} trial is presented with light off findings.

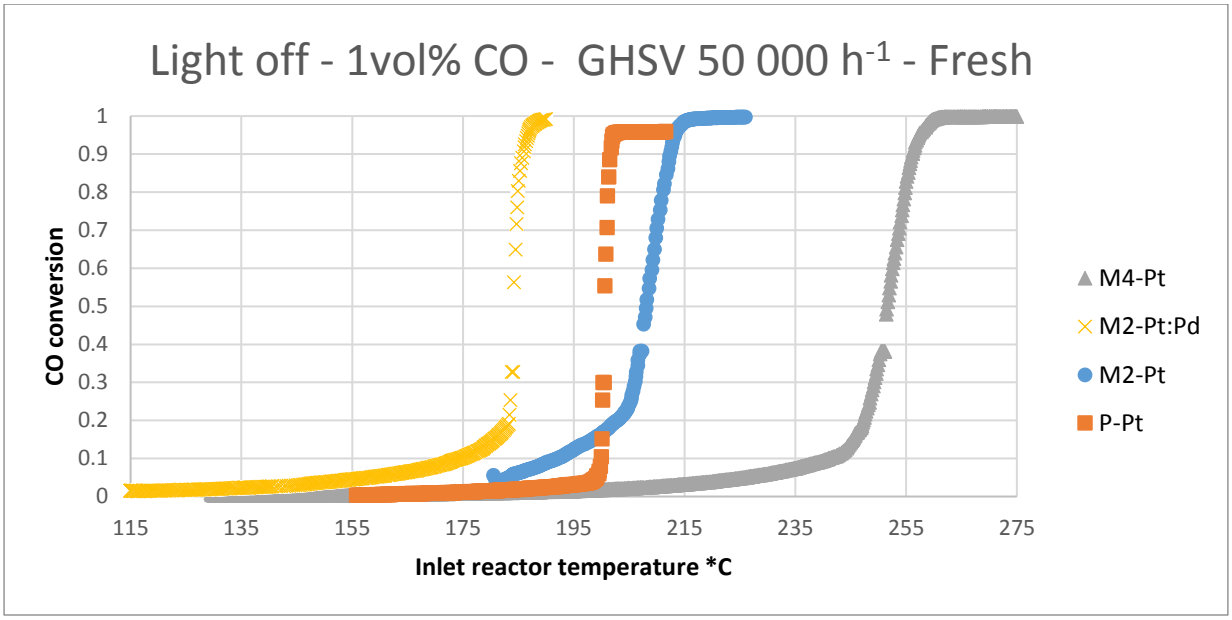

*Figure 9:1 vol% CO with an GHSV of 50 000 h-1, the different catalysts runs is specified in the legend with name as presented in the 3.3 catalyst section. The data gap on the curves is due to the **ULTRAMAT™** switching measuring range*

Increasing the GHSV decreases the light off temperature of the tested catalysts, with the exception of M2-Pt:Pd, this catalyst has the reverse behaviour:

Table 14: Catalyst light of temperatures in centigrade for fresh catalyst with 1 vol% CO, 50 000 h^{-1}. 50 corresponds to % conversion. The decrease in T_{50} temp is compared with the same samples tested with GHSV 22 000 h^{-1}.

CATALYST	T_{50} [°C]	CHANGE OF T_{50} [%]
P-PT	200	-4.8
M2-PT:PD	184	+18
M2-PT	208	-10
M4-PT	252	-3.1

Lastly, trials where done with used catalyst from real scale plants. These are interesting to compare with the thermal ageing process done on site. The samples were taken from house stock, so different process sites with varying operation conditions have an impact on the results, which are not accounted for. But nevertheless, a general aging trend on the catalysts activity vs. operation time can be confirmed:

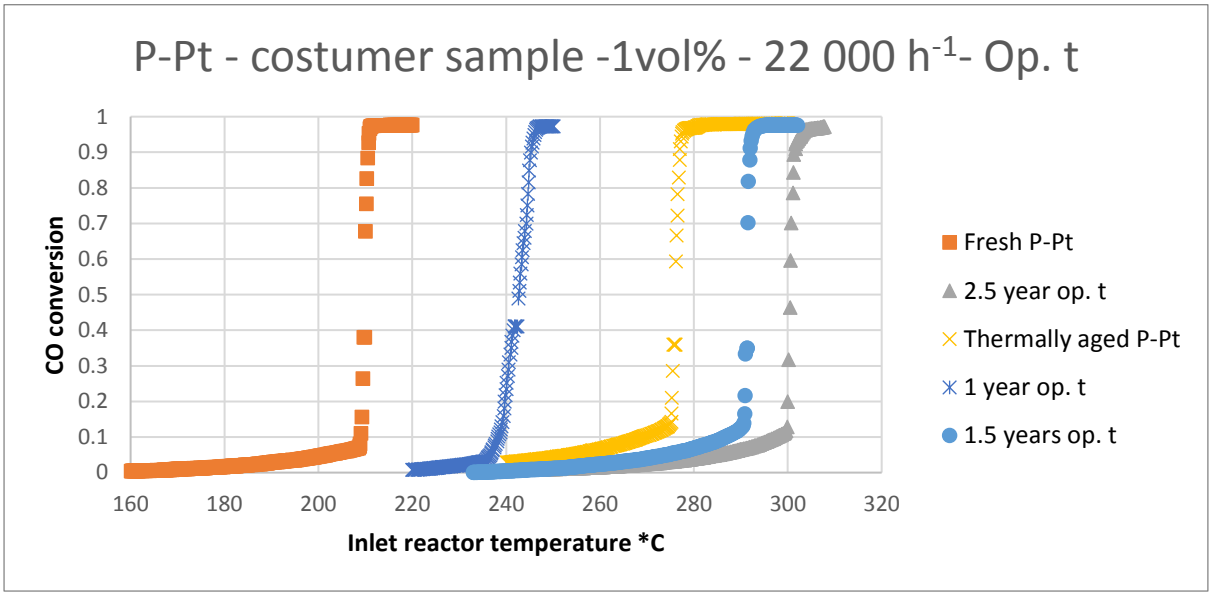

Figure 10: Costumer trials light off curves compared to the fresh- and aged sample. A decrease in activity with operation time is certain, process conditions may affect ageing as well.

Each T_{50} is summarized in the table below:

Table 15: Light off temperatures for each of the tested costumer catalysts. The fresh- and aged P-Pt light off curves are also presented for comparison.

OPERATION TIME / STATUS	T_{50} [°C]
FRESH P-PT	210
THERMALLY AGED P-PT	275
>1 YEAR OP. T	243
1.5 YEAR OP. T	291
2.5 YEAR OP. T	301

4.2 Slip values

Three different sets of slip data are presented below. One fresh and one aged at 22 000 h^{-1}, and on fresh run on 50 000 h^{-1}. All of them have DME slip values vs. outlet gas temperature. The outlet temperature is of relevance in this aspect, since the real scale plants have a maximum outlet temperature threshold which cannot be surpassed. The results reveal that it is mainly DME which slips past the catalyst bed in all the experiments.

First the fresh run on 22 000 h^{-1} is presented, see 3.4.2 for experiment method specification.

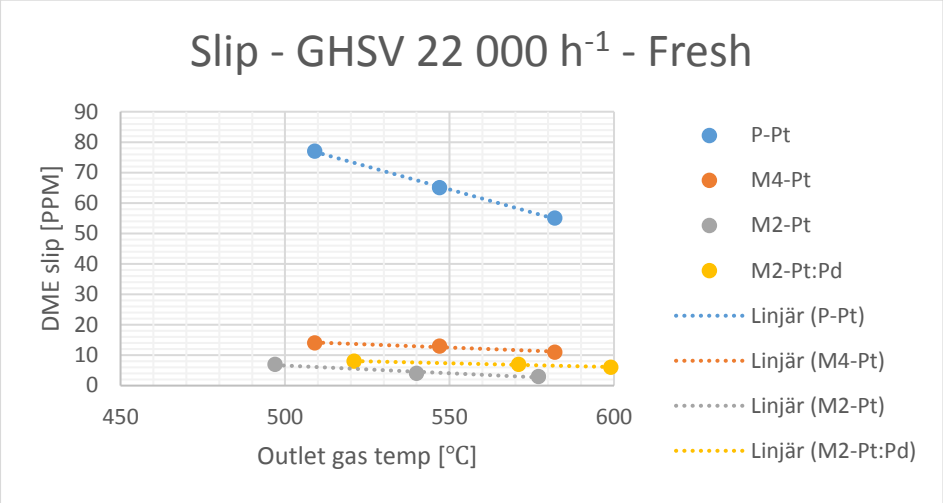

Figure 11: Slip values of DME vs. ECS outlet gas temperature at 22 000 GHSV with fresh catalysts.

Below the slip values for each catalyst is presented with, reactor furnace temperatures, outlet furnace temperatures:

Table 16:Fresh catalyst 22 000 h^{-1} slip values.

P-PT	**Reactor furnace temp** [°C]	**DME, GC** [ppm]	**T out of reactor** [°C]
	450	77	509
	500	65	547
	550	55	582
M2-Pt:Pd	**Reactor furnace temp** [°C]	**DME, GC** [ppm]	**T out of reactor** [°C]
	450	8	521
	500	7	571
	550	6	599
M2-Pt	**Reactor furnace temp** [°C]	**DME, GC [ppm]**	**T out of reactor** [°C]
	450	7	497
	500	4	540
	550	3	577
M4-Pt	**Reactor furnace temp** [°C]	**DME, GC [ppm]**	**T out of reactor [°C]**
	450	14	486
	500	13	528
	550	11	567

Then the 22 000h^{-1} aged sample:

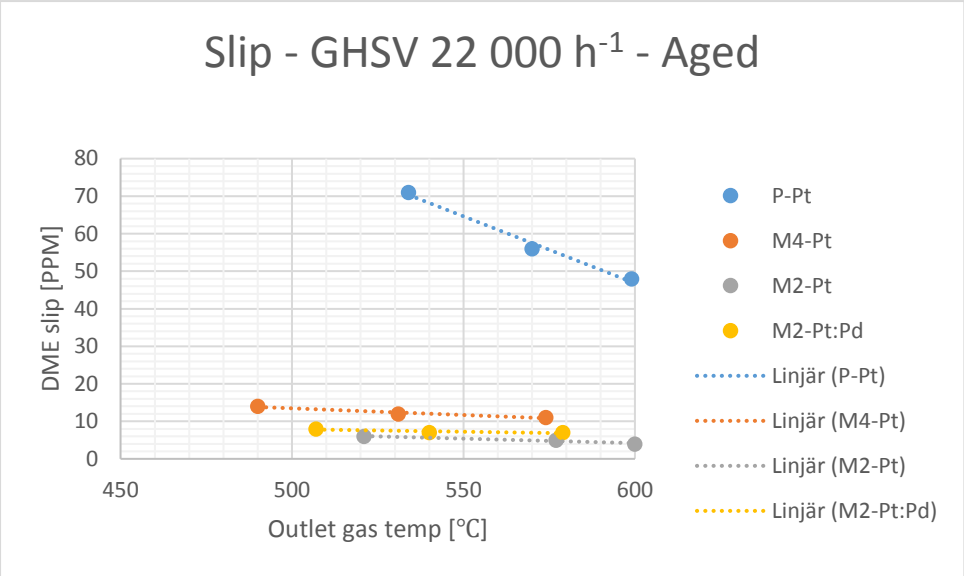

Figure 12: Slip values of DME vs. ECS outlet gas temperature at 22 000 GHSV with aged catalysts.

Tabulated slip values for 22 000 h^{-1} aged samples below:

Table 17:Aged catalyst 22 000 h^{-1} slip values.

P-PT	**Reactor furnace temp** [°C]	**DME, GC [ppm]**	**T out of reactor** [°C]
	450	71	534
	500	56	570
	550	48	599
M2-Pt:Pd	**Reactor furnace temp** [°C]	**DME, GC [ppm]**	**T out of reactor** [°C]
	450	8	507
	500	7	540
	550	7	579
M2-Pt	**Reactor furnace temp** [°C]	**DME, GC [ppm]**	**T out of reactor** [°C]
	450	6	521
	500	5	577
	550	4	600
M4-Pt	**Reactor furnace temp** [°C]	**DME, GC** [ppm]	**T out of reactor** [°C]
	450	14	490
	500	12	531
	550	11	574

And GHSV 50 000 h^{-1}:

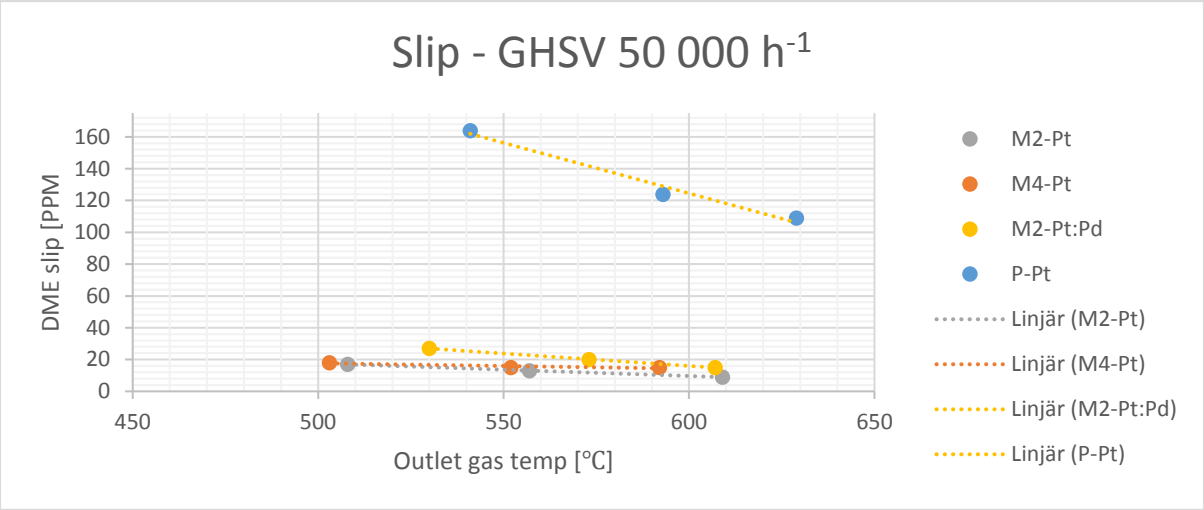

Figure 13: Slip values of DME vs. ECS outlet gas temperature at 50 000 GHSV with fresh catalysts.

With tabulated values for 50 000 h^{-1} first for pellets then monoliths:

Table 18: Fresh catalyst 50 000 slip values for P-Pt, methanol slip is also detected in these results.

P-Pt	**Reactor furnace temp** [°C]	**DME, GC** [ppm]	**MeOH, GC** [ppm]	**T out of reactor** [°C]	**DME slip increase factor**
	450	164	13	541	2.13
	500	124	8	593	1.91
	550	109	8	629	1.98

Table 19: Fresh catalyst 50 000 h^{-1} slip values.

M2-Pt:Pd	**Reactor furnace temp** [°C]	**DME, GC** [ppm]	**T out of reactor** [°C]	**DME slip increase factor**
	450	27	530	3.38
	500	20	573	2.86
	550	15	607	2.5
M4-Pt	**Reactor furnace temp** [°C]	**DME, GC** [ppm]	**T out of reactor** [°C]	**DME slip increase factor**
	450	18	503	1.29
	500	15	552	1.15
	550	15	592	1.36
M2-Pt	**Reactor furnace temp** [°C]	**DME, GC** [ppm]	**T out of reactor** [°C]	**DME slip increase factor**
	450	17	508	2.43
	500	13	557	3.25
	550	9	609	3.0

When space velocity increases, so does the slip for all catalysts. But P-Pt is the only catalyst which shows amounts of methanol slip.

The costumer samples are the final results:

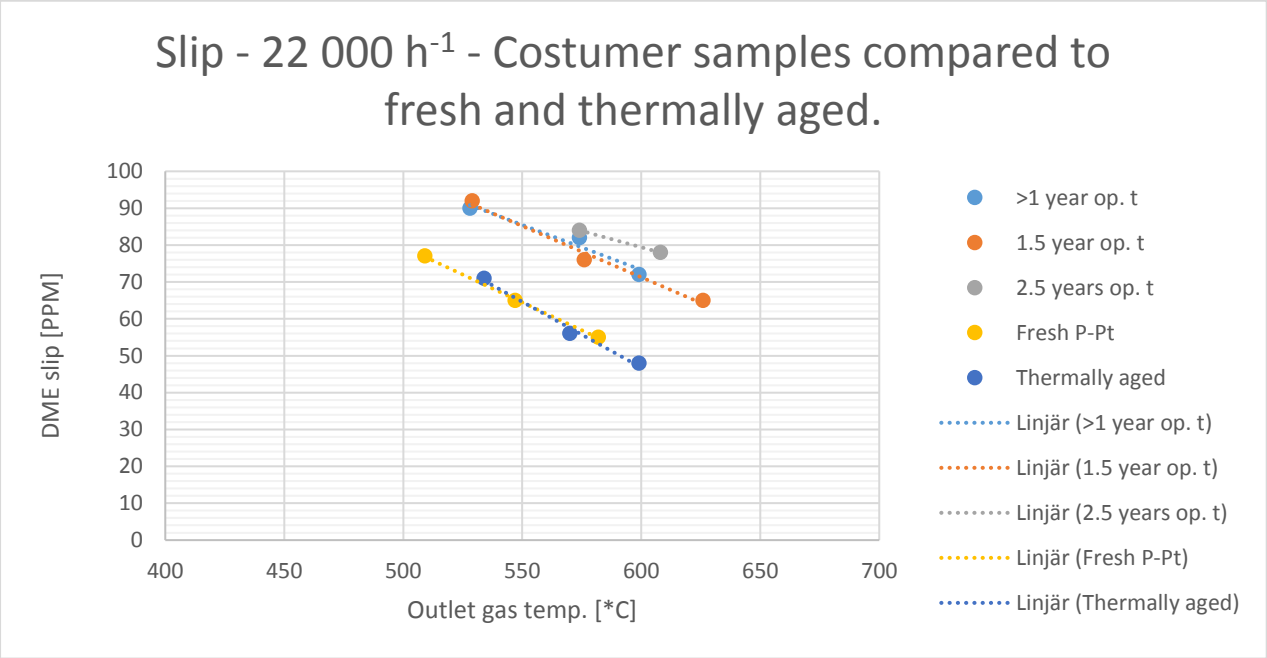

Figure 14: Costumer samples compared to the fresh and thermally aged samples pf P-Pt.

No real difference in slip values can be established between the different costumer samples. There is however a difference between the sample aged here on site, compared with the costumer samples. Indicating additional deactivation in the costumer samples, as compared with the only thermally aged sample which is produced here. The costumer samples have been operating on different plants with different conditions and might have been poisoned by a contaminant at the specific site.

Tabulated values follow for the costumer samples:

Table 20:Tabulated slip values for costumer catalyst with different operation time, the 2.5 year operation time does not have the 450 centigrade values because the reaction was deactivated at the temperature.

>1 year op. t	**Reactor furnace temp** [℃]	**DME, GC** [ppm]	**MeOH, GC** [ppm]	**T out of reactor** [℃]
	450	90	4	528
	500	82	2	574
	550	72	2	599
1.5 year op. t	**Reactor furnace temp** [℃]	**DME, GC** [ppm]	**MeOH, GC** [ppm]	**T out of reactor** [℃]
	450	92	7	529
	500	76	5	576
	550	65	3	626
2.5 years op. t	**Reactor furnace temp** [℃]	**DME, GC** [ppm]	**MeOH, GC** [ppm]	**T out of reactor** [℃]
	500	84	9	574
	550	78	3	608

There is a strong implication that there is slip of formaldehyde by at least some PPMs from the costumer samples. But as presented in section 3.2.5 no reasonable formaldehyde calibration could be made with the available equipment, and will need to be left for further studies.

5.0 Discussion

Here the result is discussed. Each experiment method will be evaluated and the different catalysts will be compared. Some experimental uncertainties and error sources will also be mentioned.

5.1 Light off comparison

Some general observations can be made across the board. Higher CO concentration causes a higher light off temperature and a higher load of active material decreases it. Independent of changes in GHSV or CO concentration the order of best activity is as load of active phase: M2-Pt:Pd > P-Pt > M2-Pt > M4-Pt. This is unexpected since the P-Pt performance should be in the same range as M4-Pt according to the previous study (1). One of the lessons learned from the previous study, was that insulation between reactor cylinder and bed of great importance to get comparable results, also in the case of P-Pt. Since insulation was poor or not present during the P-Pt trials in the previous study, this can be the cause of the light off difference when comparing results.

The monoliths in this study and the previous is more comparable. The light off for M2-Pt in the previous and this study is 220 ℃ and 215 ℃ respectively, these values is within the experiments standard deviation. This is not the case for the M4-Pt catalyst which had 240 ℃ in the previous and 259 ℃ as T_{98} in this study. A difference between the geometries is that the monoliths is slower to reach 98% conversion when the reaction is setting off. This is visualised in the light of figures above as the steepness of the light off curves.

The pellets have an almost instant conversion take off when the reaction is activated, where the monoliths takes its time to reach full conversion. This phenomenon is likely due to a less efficient heat transfer between the monoliths channels, causing a temperature difference between the inner and outer channels in the bed. The consequence is that the reaction activates in the outer layers first, and then progressing towards the centre of the monolith. Another explanation is the difference in mass transfer to the active sites between the geometries. The flow in monoliths is along straight channels without obstacles cutting of the flow, as is the case of the randomly packed bed. This could cause a turbulent flow profile in the packed bed as opposed to the monolith laminar profile. The result of this behaviour is that when the temperature in the catalyst bed reaches ignition, the conversion of CO is much faster in the packed bed compared to the monolith, causing steeper light off curves.

One would assume that a higher cell density would increase catalyst activity and thereby decrease light off temperature, instead the opposite is measured. Unfortunately, there is not much insight in the manufacturing technique of the monoliths, or the appliance of washcoat with the active material. The key to understand this behaviour is to understand the surface chemistry

Aging the catalysts results in an increased light off temperature for all catalysts except the M4-Pt which seems to be unaffected by the thermal ageing! The Light off temperature difference between the fresh and aged trial is within margin of error. A resilience towards thermal ageing would be a very preferable property and could make up for the lower activity of the M4-Pt compared with the M2-Pt and M2-Pt:Pd. However, a thorough material characterisation would have to be done before and after thermal ageing to make a reasonable conclusion regarding this.

When comparing activity, it is clearly M2-Pt:Pd that preforms best, with T_{50} 33% lower than that of the second most reactive monolith M2-Pt. Indeed, the presence of Pd seems to lower the activation of CO oxidation in the catalyst as discussed in section 2.7. However, the active compound loading is double compared to the other monoliths, which certainly also increases the activity of the catalyst.

5.2 Slip comparison

The slip experiments revealed that the main component that slips past the reactor is DME. The data also suggests that there might be a few ppm of methanol in the P-Pt and M4-Pt 22 000h^{-1} trials, but the values are; not consistent when the inlet gas temperature increases and falls below the GC calibration accuracy.

All three monoliths perform much better than P-Pt, with 5-14 times lower DME slip values on fresh trial 22 000 h^{-1}. Another difference between the geometries is that the slip difference between the temperatures is much bigger for the pellets than for the monoliths.

The catalysts were also compared in a slip experiment on 50 000 h^{-1} as presented above in the result section. The results indicate that at higher GHSV, DME slip is higher, but also the difference between the pure Pt monoliths decrease. M4-Pt improves only slightly better than M2-Pt at 500 ℃ and no real decrease in slip is measured when increasing the temperature again to 550 ℃. The M2-Pt on the other hand starts off on the same value as M4-Pt and the slip aversion improves as temperature increases, as with the 22 000 h^{-1}. M2-Pt:Pd slip values increase considerably, and most compared to the other monoliths. This behaviour is consistent with the decreased activity which is observed in the M2-Pt:Pd light off trials.

Thermal ageing does not affect the slip values in this project. Probably, the slip experiment temperatures are high enough for the sintering effects to be cancelled out by additional heat driving the reaction. At these high temperatures, there is an indication that the slip is more dependent on the GSA rather than temperature which is presented for each catalyst in section 3.3. P-Pt has the highest slip, and 5.7 times smaller GSA compared with the 230 CPSI monolith. The 230- and 400 CPSI monolith does not differ very much either in GSA or slip.

The costumer trials have as mentioned higher values of DME slip than the fresh and thermally aged on site samples. There is detectable PPMs of methanol slip from these samples, and peaks of formaldehyde was also detected.

5.2 Experimental uncertainty and sources of error

The most fundamental uncertainty of this project is the catalyst itself. If a thoroughly detailed comparison is to be made, more insight in the monolith active compound- particle size and distribution is needed. It would also be of use to do the test on several prepared samples of the same catalyst to rule out any difference in structure. During this project a light off test was made three times on the same P-Pt sample to check reproducibility of the experiment the results is presented in the figure below, this reproducibility is also compared to the previous work (1) where such experiments was made and in consistent.

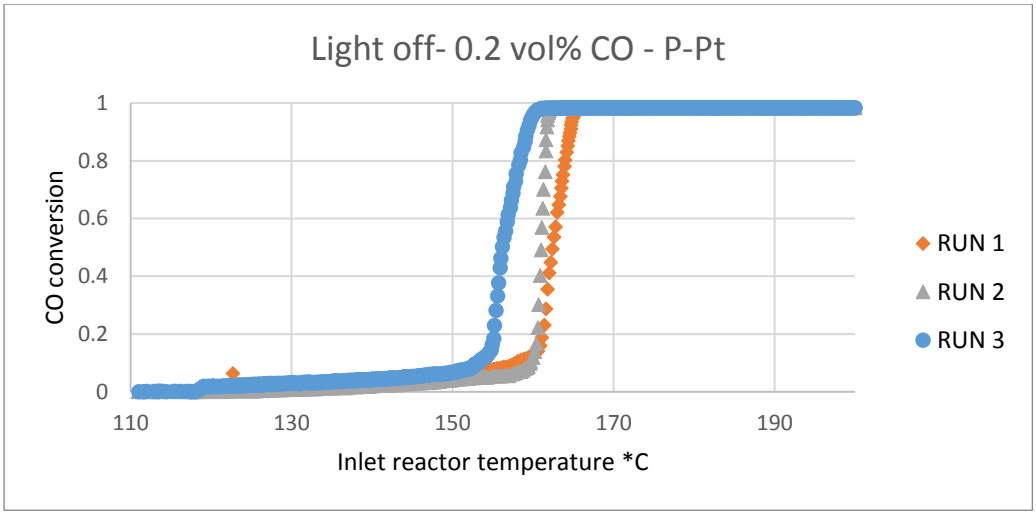

Figure 15: Three runs on the same sample with P-Pt. These results suggest that the experiment accuracy is within 5 °C, when comparing T_{50} temperatures.

The temperature control of the pilot is also somewhat unsteady. The process variable keeps oscillating around the set value, as the PID control seeks to level out the difference between set point and process variable. Also, it is only the middle and bottom heater which are programable to follow the PLC sequence and during the end of the experiments the bottom heater of the reactor furnace broke, leaving two operational heaters. This might cause for some unaccounted-for temperature gradient in the bed, and it was decided to keep a set furnace temperature, instead of a gradually increasing as with the inlet reactor temperature, which would have been the most scientific correct to avoid temperature gradients in the bed.

Another issue is with the MFCs. For the 22 000 h^{-1} experiments the DME and CO MFCs have to operate well below 10 % capacity. When operating under these conditions, the MFCs will overflow thereby deliver more gas than the set point. This was discovered during the experiment trials as the IR measured higher CO values than feed to the system.

5.3 Method suggestion

In this section a general method for technical support will be suggested. It is in JMs interest to be able to assist its customers in question regarding catalyst performance and lifetime. As the results from the customer trials of this project suggests, there is a good correlation between catalyst ignition temperature and operation time. No clear correlation between operation time and slip values can be concluded from this study, as operation variables and conditions differ from costumer to costumer. Therefore, the light off experiment of this project will be the suggested method. Further studies including surface characterization methods will be needed to make correlation regarding slip values.

The light off test is preformed accordingly:

1. Load the sample catalyst into the reactor cylinder with a layer of insulation cloth along the inner surface of the cylinder.
2. Switch on the pilot system and turn on the heat from the PLC.
3. Directly after the heat is switched on, go to sequence and switch on the sequence, which is defined below:

Table 21: Sequence steps, after the dwell time of the second step is complete, the system shuts down.

Step	Inlet temp.	Inlet temp Rate [℃/min]	Pressure [barg]	Dwell time [min]	Furnace temp.	Furnace temp Rate [℃/min]
1	110	5	1	5	110	10
2	230	2	1	1	230	2

4. The flow values also have to be put in for each MFC and Coriolis for each step according to the operators experiment inlet concentrations.

Once the sequence is started it takes about 85 min for completion of one test.

5.4 Future work

Since the last study (1), upgrades have been done to the system. Formaldehyde is now possible to feed to the system, and a GC has been installed to make individual compound specification. Unfortunately, no stable formaldehyde calibration can be made with the GC setup. The formaldehyde content can be calculated indirectly with a carbon balance, but this requires very stable calibrations of the other compounds.

6.0 Conclusion

From the results, it is quite clear that JM would benefit from changing the ECS catalyst geometry to a monolith instead of pellets. The monolith does a better job oxidizing all the compounds feed to the reactor compared to the pellets, and is more resilient to thermal aging when choosing 400 CPSI. It is quite clear that a mixture of Pd and Pt in the monolith increases the catalytic activity, and minimizes the slip, but this activity decreases as GHSV increases, as opposed to the pure Pt monoliths which shows the opposite behaviour. Still, despite this decrease in activity due to GHSV, the M2-Pt:Pd still performs better than the other monoliths, and is the recommended choice of this study

Appendix

A. Pilot process sheet

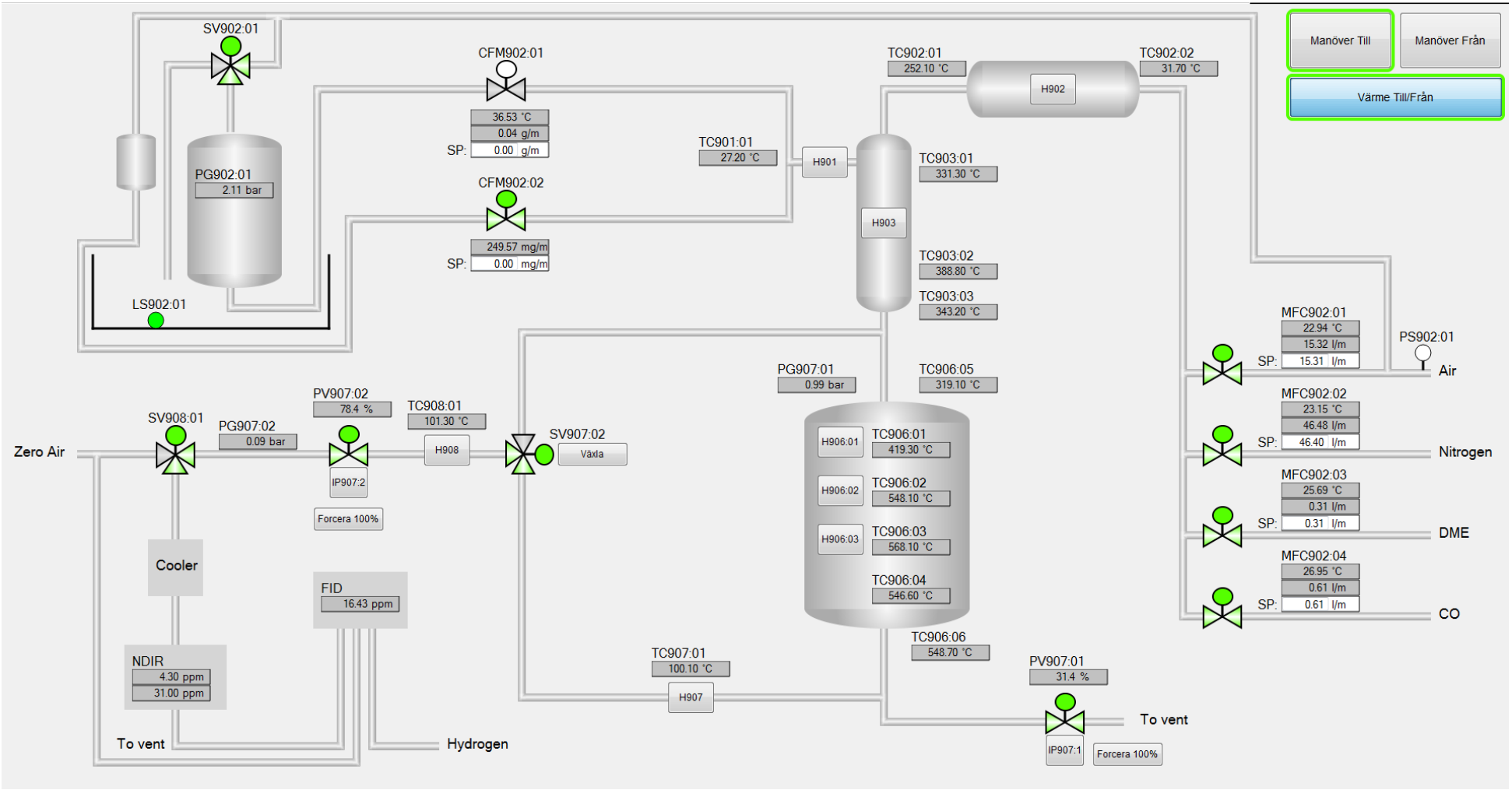

Table 22: Unit specification from the above flowsheet

PROCESS UNIT NAME	SPECIFICATION AND FUNCTION
CFM902:01	Coriolis flow meter (CFM) to control the methanol solution flow
CFM902:02	CFM to control formaldehyde solution flow
H901	Heater for liquids before vaporizer, all below heaters are PID controlled.
H902	Heater for preheater
H903	Heater for vaporizer, this heater has its set point as measured by TC906:05, reactor inlet temperature.
H906:01-3	Heaters for reactor furnace, the corresponding thermocouple is to the right of the heater symbol.
MFC902:01-4	Mass flow controllers to set flows of the process gases, named and specified in figure
PG902:01	Pressure gauge (PG) which can increase pressure in the methanol tank, higher pressure is needed for a steady flow when tank is nearly empty.
PG907:01	PG to monitor the pressure in the analytical section
PG907:02	PG to monitor the pressure in the reaction section
PV907:01	Pressure valve (PV) to set and control reaction section pressure
PV907:02	PV to set and control analytical section pressure
SV902:01	Switch valve (SV) this valve was never used during the project
SV907:02	SV that controls the bypass of the reactor when engaged, reaction exhaust is lead to the analytical section. When disengaged inlet gas mixture is analysed instead.
SV908:01	SV that is operational from the NDIR, when a zero calibration is made, this SV is disengaged, so zero gas can flow to the instrument instead of process gas
TC901:01	Thermocouple (TC) at union of liquids, measures temperature in centigrade before vaporizer
TC902:01-2	TC before and after preheater
TC903:01-3	TC stages in the vaporizer
TC906:01-6	TC stages reactor, placement as in figure.

TC907:01	TC in pipe between reactor and analytical section
TC908:01	TC at analytical section furnace

B. Methanol solution preparation

1. Methanol (99wt%~ 100wt%) solution was collected from a bulk tank on site.
2. 2.5 kg was the target weight for the water in the solution.

$$2500\ g\ H_2O \leftrightarrow \frac{2500g}{18.016\frac{g}{mol}} = 138.77\ mol$$

$$\frac{n_{MeOH}}{n_{MeOH} + n_{H_2O}} = \frac{n_{MeOH}}{n_{MeOH} + 138.77\ mol} = 0.0500 \quad \leftrightarrow \quad n_{MeOH} = 7.30mol \leftrightarrow m_{MeOH} = 234.0\ g$$

$$m_{tot} = 2500g + 234.0\ g = 2734\ g$$

3. A plastic vessel was zeroed on a scale and the methanol was poured into the vessel on the scale until 234 g.
4. Then distilled water was poured in the vessel until it showed 2734 g.

C. Coriolis calibration data

Table 23: Formaldehyde data points

Data point	Coriolis SP in PLC (mg/min)	Time[1)] (min)	Start mass (g)	End mass (g)	Diffence mass (mg)	Mass $flow_{act}$ (mg/min)	Diff. set/act (%)
1	25.00	118	68.541	71.480	2939.000	24.907	-0.37
2	75.00	63	71.4800	76.2480	4768.000	75.683	0.91
3	150.0	63	76.248	85.579	9331.000	148.111	-1.26
4	250.0	65	85.579	101.517	15938.000	245.200	-1.92

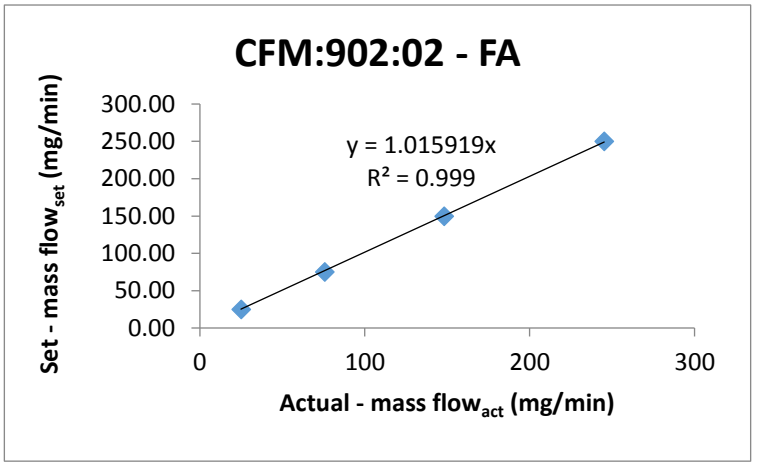

Figure 16: Linearization of formaldehyde data points

Table 24: MeOH data points

Data point	Coriolis SP in PLC (g/min)	Time[1)] (min)	Start mass (g)	End mass (g)	Diffence mass (g)	Mass $flow_{act}$ (g/min)	Diff. set/act (%)
1	3.0	60	203.030	382.700	179.670	2.995	-0.18
2	6.0	28	203.750	369.860	166.110	5.933	-1.13
4	12.0	16	203.7100	385.170	181.460	11.341	-5.49
5	15.0	12	203.700	382.600	178.900	14.908	-0.61

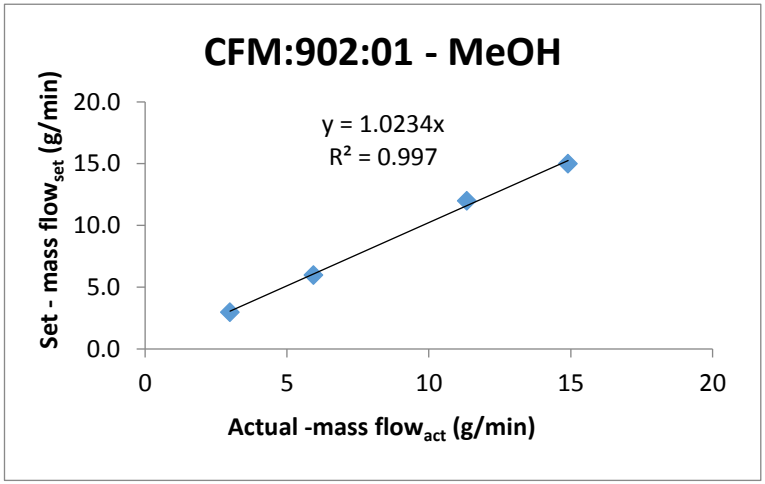

Figure 17: Linearization of MeOH data points

D. MFC calibration data

Table 25: Air MFC data points.

MFC 1 (air)		
Set point (Nl/min)	Actual value (Nl/min)	Diff. (%)
10	10.03	0.3
20	20.05	0.3
30	30.083	0.3
40	40.18	0.4
50	50.1	0.2

Table 26: Nitrogen MFC data points.

MFC 2 (N_2)		
Set point (Nl/min)	Actual value (Nl/min)	Diff. (%)
40	39.66	-0.85
80	78.72	-1.6
120	117.36	-2.2
160	155.72	2.675
200	194.36	-2.82

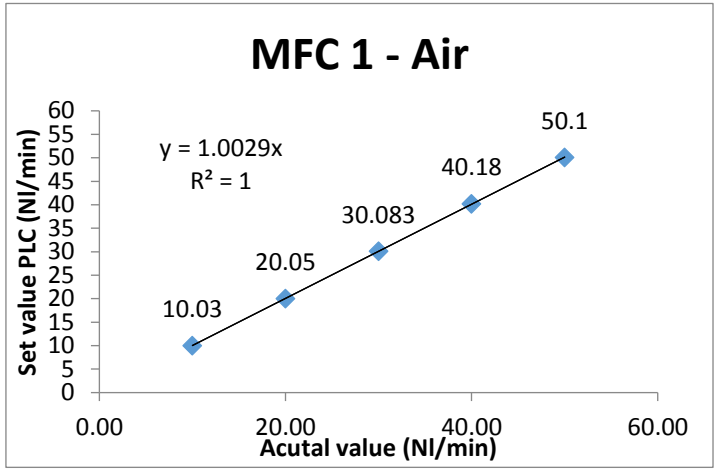

Figure 18: Linearization of ait MFC data points

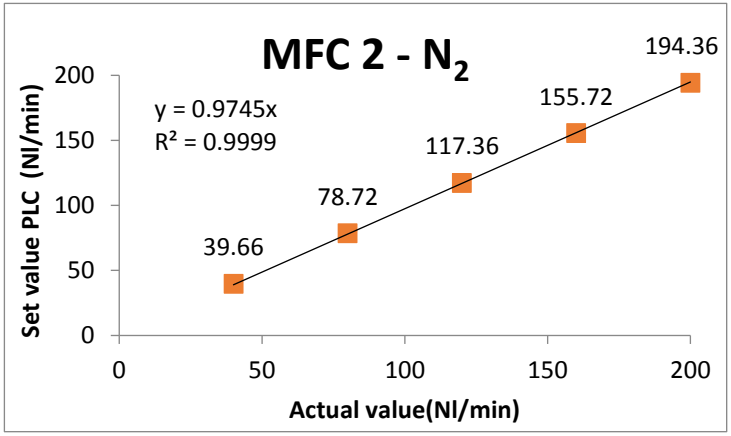

Figure 19: Linearization of nitrogen MFC datapoints.

Table 27: DME MFC data poins.

MFC 5 (DME)		
Set point (Nml/min)	Actual value (Nml/min)	Diff. (%)
300	315.34	5.1
480	503.11	4.8
650	674.97	3.8
830	853.21	2.8
900	924.95	2.8

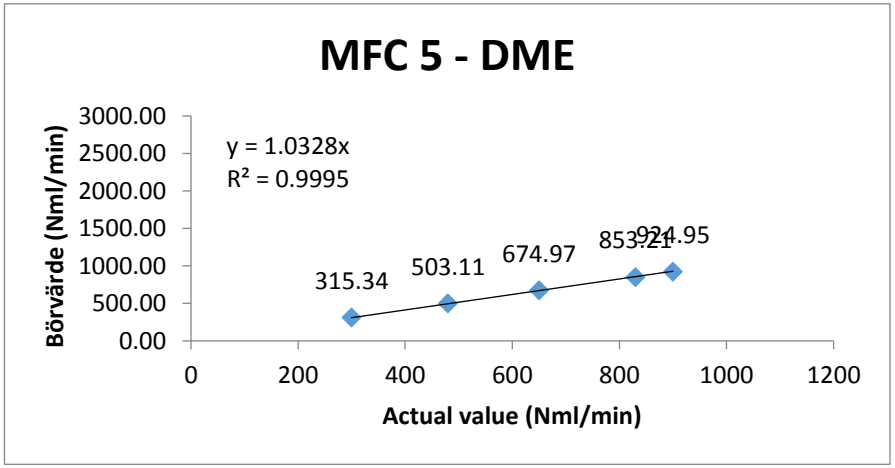

Figure 20: Linearization of DME MFC data.

Table 28: CO MFC data points.

MFC 6 (CO)		
Set point (Nl/min)	Actual value (Nl/min)	Diff. (%)
0.5	0.53896	7.8
1.5	1.5519	3.5
2.5	2.5662	2.6
3.5	3.5845	2.4
4.5	4.6084	2.4

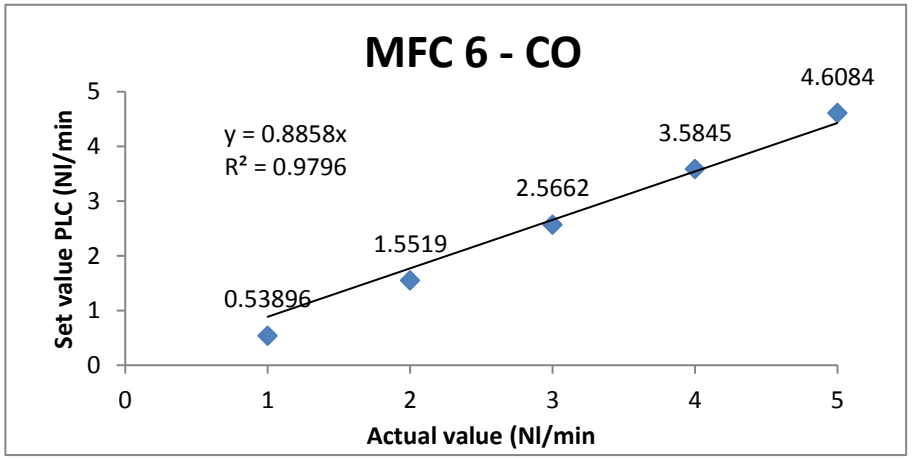

Figure 21: Linearization of CO MFC data.

E. Calibration gases used for calibration in the gas chromatograph

Table 29: Gas chromatograph calibration, each gas was measured at least 10 times, when calibrating.

CALIBRATION	GAS NAME	NO OF GC INJECTIONS	GAS COMPOSITION (PPM)							
			METHYL FORMATE	METHANOL	CARBON MONOXIDE	CARBON DIOXIDE	DIMETHYL ETHER	METHYLAL	NITROGEN (%)	OXYGEN (%)
LC1	CALIBRATION GAS 1	15	0.00	1000.0	3013.0	992.8	2032.0	0.00	88.3	11.0
LC2	CALIBRATION GAS 2									
LC3	CALIBRATION GAS 3	20	0.00	5000.0	20 000.0	0.0	5000.0	0.00	86.0	11.0
LC4	CALIBRATION GAS 5	13	0.00	1000.0	10 000.0	5000.0	1000.0	0.00	91.3	7.0
LC5	CALIBRATION GAS 8									
LC6	CALIBRATION GAS 9									
LC7	CALIBRATION GAS 11	15	10.10	999.6	50.8	254.0	253.8	20.28	99.8	0.0
[LC8]	CALIBRATION GAS 12*	-	50	2000	500	100	500	0	>99.67	0.0
LC9	CALIBRATION GAS 13	10	203.70	502.4	1000.2	200.7	0.0	302.6	99.8	0.0

*Calibration gas 12 was only used for **ULTRAMAT™** IR calibration

F. Average peak areas and the corresponding concentration linearization in figures

Table 30: Peak areas and concentrations for methanol in the methanizer detector

METHANOL (MeOH) - Methanizer	
Peak area (mV*s)	Concentration (vol-%)
0.00	0.00
206.72	0.05
578.20	0.10
621.53	0.10
2663.909569	0.5

Table 31: linearization of above table values

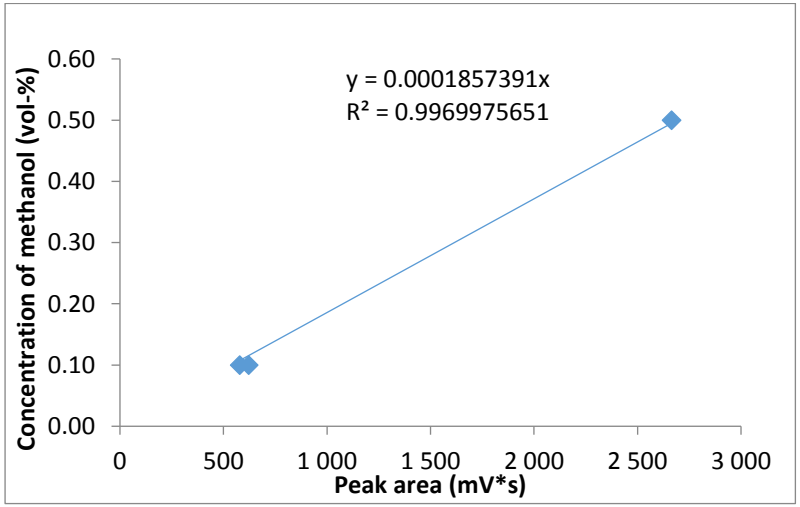

Table 32: Peak areas and concentrations for methanol in the FID detector

METHANOL (MeOH) - FID	
Peak area (mV*s)	Concentration (Vol-%)
0.00	0.00
189.52	0.10
204.86	0.10
850.54	0.50

Table 33: linearization of above table values

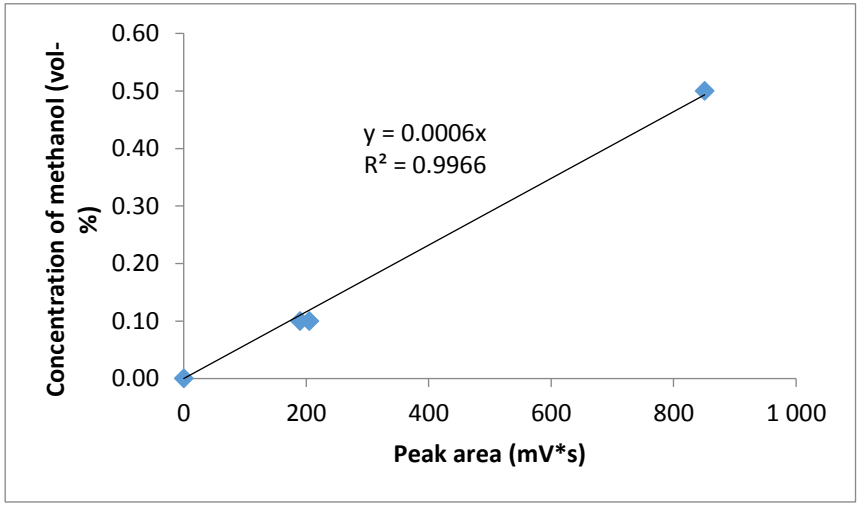

Table 34: Peak areas and concentrations for dimethyl ether in the methanizer detector

DIMETHYL ETHER (DME) - Meth	
Peak area (mV*s)	Concentration (Vol-%)
0.00	0.00
1053.781	0.10
1886.77	0.20
57.56	0.025
5017.97	0.50

Table 35: Linearization of above tables values

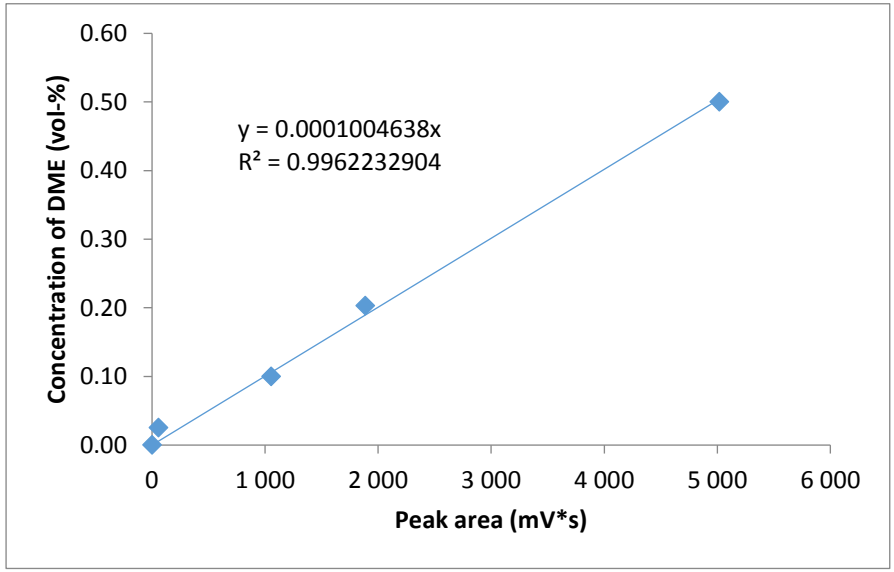

Table 36: Peak areas and concentrations for dimethyl ether in the FID detector

DIMETHYL ETHER (DME) - FID	
Peak area (mV*s)	Concentration (Vol-%)
0.00	0.00
279.45	0.10
496.94	0.20
1320.19	0.50

Table 37: Linearization of above tables values

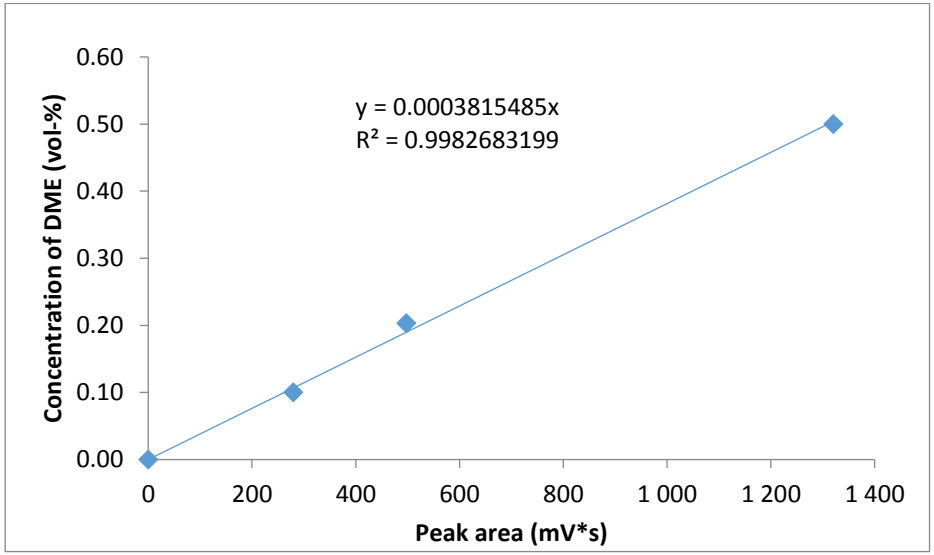

Table 38: Peak areas and concentrations for CO in the methanizer detector

CARBON MONOXIDE (CO) - Methanizer	
Peak area (mV*s)	Concentration (Vol-%)
0.00	0.00
28.00	0.0051
1084.23	0.30
5831.68	2.00

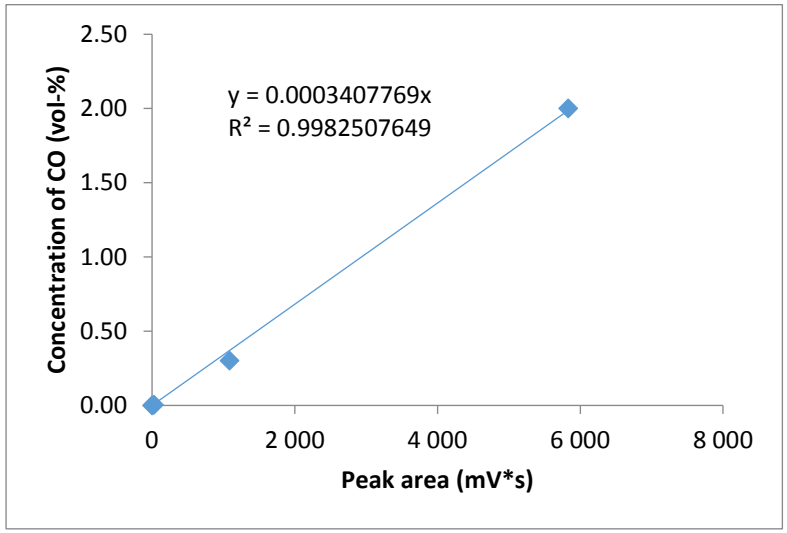

Table 39: Peak areas and concentrations for CO_2 in the methanizer detector

CARBON DIOXIDE (CO2) - Meth	
Peak area (mV*s)	Concentration (Vol-%)
0.00	0.00
497.75	0.10
2360.06	0.50

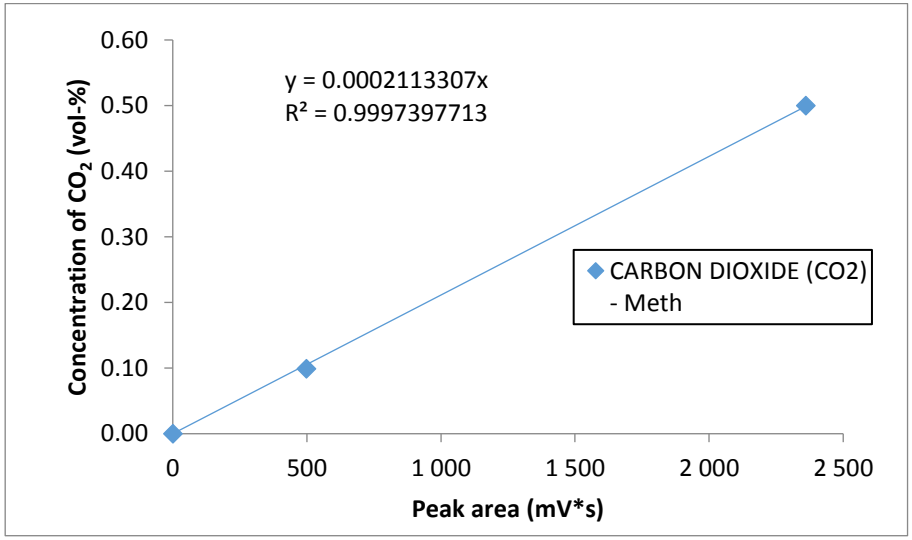

G. Catalyst geometry calculations

Pellets:

diameter = 4.7 mm

$A_{surface} = 4\pi r^2 = \pi d^2$ per pellet

The reactor volume is calculated with respect to the diameter decrease due to insulation

$$V_{Reactor} = \frac{\pi \cdot d^2}{4} \cdot h = \frac{\pi \cdot 0.038^2 m^2}{4} \cdot 0.140\ m = 1.59 \cdot 10^{-4}\ m^3$$

The reactor cylinder was filled with pellets to 140 mm bed height and weighed. One pellet weight was estimated by weighing several then taking the average. The full reactor volume of pellets was divided with the weight of a single pellet to estimate the number of pellets in one reactor.

$$m_{pellets,reactor} = 93.6\ g$$

$$m_{\ pellet} = \frac{0.115\ g + 0.122\ g + 0.090\ g + 0.095\ g + 0.137\ g}{5} = 0.11\ g$$

$$n_{pellets,reactor} = \frac{m_{pellets,reactor}}{m_{pellet}} \sim 850\ st/reactor$$

$$GSA_{pellet,reactor} = \frac{A_{surface} \cdot n_{pellets,reactor}}{V_{Reactor}} = 371 \frac{m^2}{m^3} = 9.43\ in^2/in^3$$

References

1. **Andersson Maria.** *Honeycomb based ECS for turbocharged FA plant.* Perstorp : --, 2017. --.

2. **Corning Incorporated.** Ceramic Catalyst Supports for Gasoline Fuel. [book auth.] Suresh T. Gulati. *Strucktured Catalysis and Reactors.* New York : Marcel Dekker, 1998.

3. **Chorkendorff, I. and Neimantsverdriet, J.W.** *Concepts of Modern Catalysis and Kinetics.* Weinheim : Wiley-VCH Verlag GmbH & Co. KGaA, 2007. ISBN 978-3-527-31672-4.

4. **Moulijn, Jacob A., Makkee, Michiel and Diepen, Annelies E. Van.** *Chemical Process Technology.* The Netherlands : John Wiley & Sons Ltd, 2013. ISBN 9781444320251.

5. ***Johnsson Matthey Formaldehyde process upgrades.*** **[Online] Johnson Matthey, - - 2017. [Cited: 26 04 2018.] http://www.jmprotech.com/jm-formox-formaldehyde-process-upgrades.**

6. The FORMOX™ Process. ***Johnsson Matthey - FORMOX™.*** **[Online] Johnsson Matthey, - - 2018. [Cited: 20th September 2018.] http://www.jmprotech.com/jm-formox-formaldehyde-process.**

7. Johnsson Matthey - FORMOX™. ***Turbocharger and steam utillization.*** **[Online] Johnsson Matthey, - - 2018. [Cited: 20th September 2018.] http://www.jmprotech.com/jm-formox-turbocharger-and-steam-utilization.**

8. Roberts, George W. ***Chemical Reactions and Chemical Reactors.*** **United States of America : John Wiley and Sons Inc., 2009. ISBN-13 978-0471-74-2203.**

9. [Online] https://lost-contact.mit.edu/afs/nada.kth.se/amdlinks/pkg/femlab/3.1x/doc/chemmodlib/chem31_ml_mass2.htm.

10. Cybulski, Andrzej and Moulijn, Jacob A. The Present and the Future of Structured Catalysts - An Overview. ***Structured Catalysts and Reactors.*** **New York : Marcel Dekker Inc., 1998.**

11. ***FEMLAB User's Manual - Monolithic Reactor.*** **COMSOL, Inc. . s.l. : COMSOL, Inc. , 2001, Vol. version 2.2.**

12. ***Low-temperature catalysis for VOCs removal in technology andapplication: A state-of-the-art review.*** **Zhanga, Zhixiang, Jiang, Zheng and Shangguana, Wenfeng. pp. 270 - 278, China , UK : Elsevier, 2015, Vol. 264. https://doi.org/10.1016/j.cattod.2015.10.040.**

13. ***Platinum supported on highly-dispersed ceria on activated carbon forthe total oxidation of VOCs.*** **Z. Abdelouahab-Reddama, R. El Mailb, F. Colomaa, A. Sepúlveda-Escribanoa. pp. 87 - 94, Spain , Morocco : Elsevier, 2015, Vol. 494. https://doi.org/10.1016/j.apcata.2015.01.026.**

14. ***Tuning/exploiting Strong Metal-Support Interaction (SMSI) in Heterogeneous Catalysis.*** **Chun-Jern Pan, Meng-Che Tsai, Wei-Nien Su , John Rick , Nibret Gebeyehu Akalework, AbiyeKebede Agegnehu, Shou-Yi Cheng, Bing-Joe Hwang. pp. 154 - 186, Taiwan : Elsevier, 2017, Vol. 74. ISSN1876-1070.**

15. Herbschleb, Cornelis Thaddeus. Doctoral Thesis. ***ReactorSTM : imaging catalysts under realistic conditions.*** **Leiden, The Netherlands : Faculty of Science, Leiden University, 2011. ISBN 9789085930983.**

16. ***Mechanisms of catalyst deactivation.*** **Bartholomew, Calvin H. -, Provo, USA : Elsevier, 2001, Vol. 212. https://doi.org/10.1016/S0926-860X(00)00843-7.**

17. Duprez, Jacques Barbier Jr and Daniel. Oxidation of CO and Hydrocarbons in Exhaust Gas Treatments. ***Handbook of Advanced Methods and Processes in Oxidation Catalysis.*** **Weinheim : WILEY-VCH Verlag GmbH & Co. KGaA, , 2015 .**

18. ***On highly active partially oxidized platinum in carbon monoxide oxidation over supported platinum catalysts.*** **E.M.C. Alayon a, J. Singh a, M. Nachtegaal b, M. Harfoucheb, J.A. van Bokhovena. 263, Switzerland : Elsevier, 2009. ISSN: 0021-9517.**

19. ***CO Oxidation as a Prototypical Reaction for Heterogenous Processes.*** **Hans-Joachim Freund, * Gerard Meijer,* Matthias Scheffler,* Robert Schlçgl,* and. 43, Berlin : WILEY-VCH Verlag GmbH & Co. KGaA, , 2011, Vol. 50. DOI: 10.1002/anie.201101378.**

20. ***Adaptive Global Carbon Monoxide Kinetic Mechanism over Platinum/Alumina Catalyst.*** **Christopher Depcik, Sudarshan Loya , Anand Srinivasan , Travis Wentworth and Susan Stagg-Williams. 2, Lawrence, Kansas : MDPI, 2013, Vol. 3. ISSN 2073-4344.**

21. ***Kinetic and mechanistic study of bimetallic Pt-Pd/Al2O3 catalysts for CO and C3H6 oxidation.*** **Melanie J. Hazletta, Melanie Moses-Debuskb, James E. Parks, Lawrence F. Allard, William S. Eplinga. pp. 404 - 417, United states of america : Elsevier, 2016, Vol. 202. https://doi.org/10.1016/j.apcatb.2016.09.034.**

22. ***Partial oxidation of dimethyl ether over various supported metal catalysts.*** **Shizhong Wang, Tatsumi Ishihara, Yusaku Takita. 1-2, s.l. : Elsevier, 2002, Vol. 228. https://doi.org/10.1016/S0926-860X(01)00985-1.**

23. ***Progress in research on catalysts for catalytic oxidation of formaldehyde.*** **Bingyang Bai, Qi Qiao, Junhua Li, Jiming Hao. Beijing : Elsevier, 2016, Vol. 37. https://doi.org/10.1016/S1872-2067(15)61007-5.**